Development of electronic nose using chemiresistive percolation network gas sensor based on conducting polymers

Åbo Akademi University

Faculty of Science and Engineering

Rodney Salazar

Excellence in Analytical Chemistry Erasmus Mundus Joint Master Degree

Co-funded by the Erasmus+ Programme of the European Union

Master's programme in Excellence in Analytical Chemistry

Degree project in Analytical chemistry, 30 credits

Supervisor: Docent Dr. Tomasz Sokalski (Åbo Akademi University)

Co-supervisor: Dr. Agnes Heering (University of Tartu)

August 2023

Preface

This master's thesis presents the research conducted as a requirement for the Erasmus Mundus joint master's degree programme-EACH (Excellence in Analytical Chemistry) at the Laboratory of Science and Engineering, Åbo Akademi University's Aurum Building.

I wish to express my sincere gratitude to the individuals who made this research possible. Firstly, I owe a debt of thanks to my thesis supervisor, Dr. Tomasz Sokalski, for the trust and autonomy he granted me throughout this project. His support allowed me to develop my problem-solving skills and gain confidence in my abilities. I deeply value the freedom he gave me to explore diverse approaches and implement my own ideas.

I am also grateful to my thesis co-supervisor, Dr. Agnes Heering, for providing valuable editing comments that significantly improved my writing.

My heartfelt appreciation goes to all my teachers and classmates at EACH, who played a pivotal role in making this year one of the most productive and transformative periods of my life. Your presence not only enriched my knowledge in chemistry but also provided me with valuable insights into different cultures, thanks to your constant support and guidance.

Special recognition is owed to Prof. Ivo Leito and Prof. Johan Bobacka for their exceptional leadership, which made the EACH program an outstanding and well-organized academic journey. Their commitment to excellence has profoundly influenced my academic and professional growth.

To my parents, Filma and Ben, I am incredibly grateful for being my unwavering support system throughout my time in Estonia and Finland. Your encouragement and love have been invaluable to me.

May I present to you the paper the signifies the culmination of my EACH journey.

Rodney Cuenca Salazar 

Abstract

A method of producing poly(3,4-ethylenedioxythiophene) (PEDOT) explosive percolation (EP) gas sensor with ultra-fast response and recovery time has been developed by Robiños et. al. Due to its novelty full understanding of its the mechanism and validating its performance are still lacking to utilized for application such as electronic nose. To improve reproducibility of the method a modification called pulsed galvanostatic polymerization was employed wherein removal of interdigitated electrode from the solution was eliminated such method also led to discovery that electrochemical condition or p-doping is not needed to achieve a fast response, fast recovery, and n-type gas sensor for ammonia. In another effort to improve reproducibility of the method electropolymerization via in-situ conductance monitoring was also employed, the large initial resistance of the system however prevents monitoring of percolation region.

Method of production of EP gas sensor was also tested in ionic liquid and other conducting polymer such as PANI. Performance of produced sensors were assessed through various performance characteristics such as gas response, linearity, limit of detection, recovery time and sensitivity. Selected sensors were then used as chemiresistor for an electronic nose system which provided intermediate accuracy for classifying solvents.

Overoxidation as a possible explanation for peculiar n-type behavior of PEDOT EP gas sensor was also proposed.

Keywords: explosive percolation, gas sensor, electronic nose, conducting polymer, ionic liquid, PEDOT

Glossary of terms and abbreviations

AC	alternating current
Ag	silver
AgCl	silver chloride
$BMIMPF_6$	1-butyl-3-methylimidazolium hexafluorophosphate
CE	counter electrode
CP	conducting Polymer
CV	cyclic voltammetry
d	diameter
DC	direct current
DC	direct current
E	potential
EDOT	3,4-ethylenedioxythiophene)
E_{EP}	electropolymerization potential
EMIMFSI	1-ethyl-3-methylimidazolium bis(trifluoromethylsulfonyl)imide
EN	electronic nose
e-nose	electrical nose
EP	explosive percolation
I	current
i_d	current across deposited CP
IDE	interdigitated electrode
i_f	faradaic current
LOD	limit of detection
MeCN	acetonitrile
N_2	nitrogen gas
PANI	polyaniline
PARC	pattern recognition and classification
PEDOT	poly(3,4-ethylenedioxythiophene)
Ppy	polypyrrole
Q_{EP}	electropolymerization charge
R	sensor response
R_a	resistance in air
RE	reference electrode

R_g	resistance upon exposure to analyte gas
$TABClO_4$	tertbutyl ammonium hexafluorophosphate
Vd	drain potential
VOC	volatile organic compounds
WE	working electrode

Table of Contents

1. Introduction

Biology has always been a great source of inspiration to solve human societal and industrial challenges, through biomimicry we carefully study biological processes and draw inspiration from them. An example is how the kingfisher beak inspired Japan's bullet train [1,2]. For analytical chemists, the sense of smell is interesting chemical phenomenon in nature. Human olfactory cells located high up in the nasal passage, act as receptors to volatile organic compounds (VOCs) and the response forms a pattern that is being processed in the brain. This mechanism helps us take appropriate response from stimulus around our environment and an is an inspiration for so called electronic nose or e-nose (see Figure 1) [3].

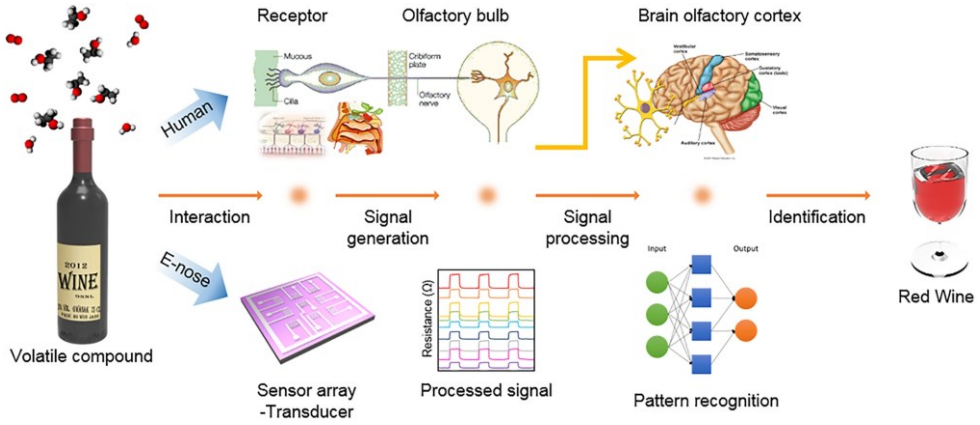

Figure 1. Comparison between human nose and E-nose. Adapted from [4].

The use of e-nose has been reported in a wide range of applications such as environmental monitoring, medical diagnostics, recognition of natural products, process monitoring, food quality assurance, automotive/aerospace applications, detection of explosives and cosmetics/fragrances [5–12].

Conducting polymer, a versatile material with interesting electrical properties and high environmental stability has already been implemented as a sensing unit in several e-nose systems [13]. Most of these applications use a thin film of conducting polymer based chemiresistor for gas sensing in which it limits the interaction between the polymer and gas molecules as the polymer thickness increases because of increasing inter-domain space [14]. Castell et. al, reported an improved sensitivity of these sensors through a conducting polymer percolation network on glass substrate [15,16]. Percolation region in the context of conducting polymer based chemiresistor is a region between the insulating phase and the conducting phase caused by at least one interconnected cluster across medium.

On the other hand, explosive percolation network gas sensor based on conducting polymer has been reported by Robiños et. al, which is a further improvement from the previous method and/or process [17].

Improved sensitivity however comes at a cost, it suffers from reproducibility issues due to inherent randomness of the conducting polymer network and small variation into the network has large effect on its conductance [17,18].

In this study, various techniques were employed to improve repeatability of manufacturing explosive percolation gas sensors. Performance characteristics were used to assess its fitness as gas sensor and as electronic nose sensing unit.

2. Review of related literature

2.1. **Chemiresistors**

Chemiresistors are chemical sensors which utilize the change of their conductance as sensing information. The selective layer interacts with a gas sample, this interaction leads to change in contact resistance, bulk resistance and interface resistance (see Figure 2) [19]. To monitor these changes a constant current or potential is applied on the sensor and potential or current is measured as a signal which is then converted to electrical resistance as the final signal output [20].

These sensors are simple to prepare and with simple instrumentation typically using interdigitated electrodes (IDE) (see Figure 3). Interdigitation enables a wide contact area between electrode in a limited space and promotes effective charge transport [19].

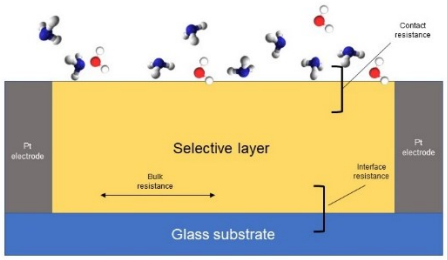

Figure 2. General configuration of chemiresistor

Figure 3. An interdigitated electrode. The gray pattern is a conducting material (usually gold or platinum) embedded in an insulating substrate (usually glass).

2.2. **Conducting polymer (CP)**

Also called conductive polymers, conjugated conductive polymers or organic polymeric conductors are materials that are intrinsic conductors. They are mainly composed of carbon and

hydrogen with some heteroatoms like nitrogen and sulfur. This conductivity arises from extended and delocalized conjugation from overlapping π-electrons [21].

2.2.1. PEDOT

One of the derivative of polythiophene (PTs) class of CPs, poly(3,4-ethylenedioxythiophene) PEDOT is one of the most common materials for chemiresistive gas sensing because its ease of fabrication, high conductivity, room temperature operation and stability [22] [23].

PEDOT can be prepared via electrochemical polymerization methods. These include potentiostatic polymerization, galvanostatic and cyclic voltammetry techniques [21] . When a certain oxidation potential is applied to the electrode substrate EDOT, the monomers of PEDOT are rapidly oxidized to generate a radical cation, which then attacks another abundant monomer molecule in the solution to form a dimer radical cation. The dimer is further oxidized and forms a positively charge cationic group, further repetition of this process yields a PEDOT conjugated chain. To balance the positive charge an anion (A^-) called dopant enters the polymer chain as illustrated in Figure 4 [24].

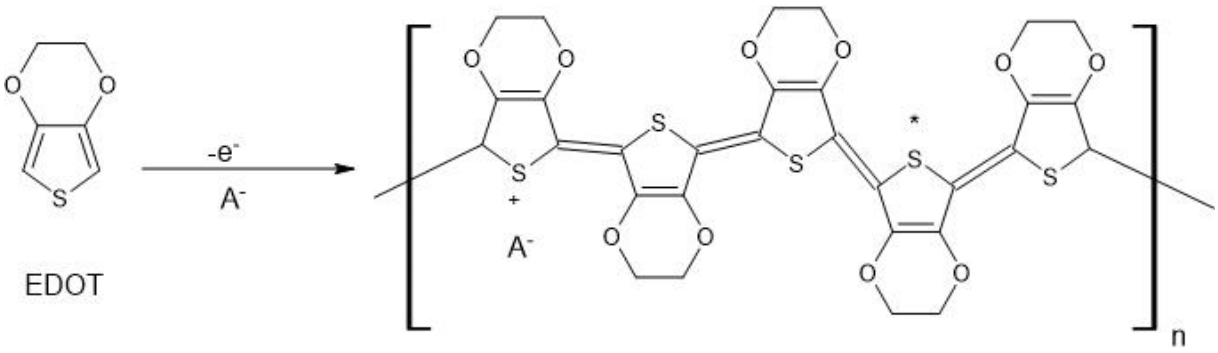

Figure 4. Proposed mechanism for electrochemical polymerization of EDOT into PEDOT

2.2.2. PANI

A result of oxidative polymerization of aniline, polyaniline (PANI) chains are composed of two structural units [B-NH-B-NH] and [B-N=Q=N$^-$] which are reduced and oxidized repeating units respectively, B-denotes benzoid ring while Q denoted a quinod ring [25]. There are three oxidation states of PANI chain, these include completely reduced leucomeraldine (LED), semi-oxidized emeraldine (EB) and fully oxidized pernigraniline base (PAB) (see Figure 5) [26].

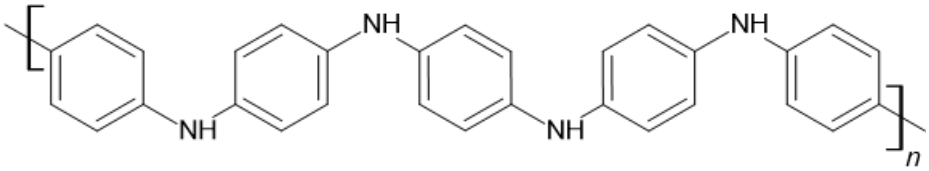

LEB

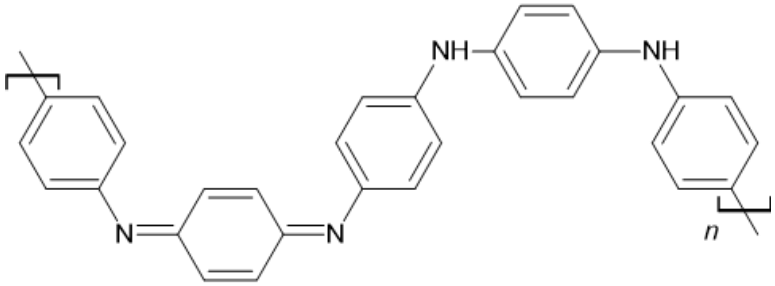

EB

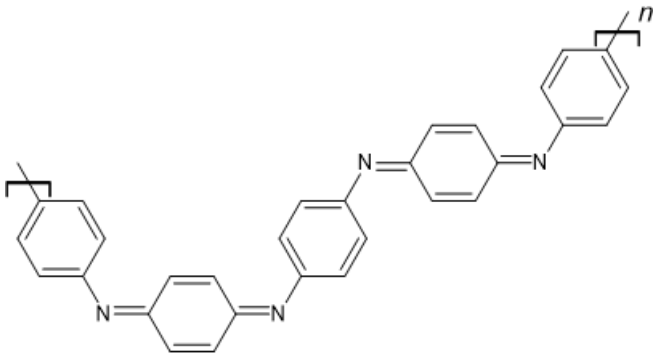

PAB

Figure 5. Three oxidation states of PANI chain: LEB, EB and PAB.

PANI, in its EB salt form, has interesting electrical conductivity. In acidic condition, EB is doped and it is conductive. In basic condition on the other hand EB is in dedoped form and is insulating. Its ability of switching between conducting and insulating forms makes it ideal for acid/base gas sensing of compounds [27].

2.3. **Electrochemical methods**

Conducting polymer can be deposited onto electrode material using various electrochemical waveforms these include potentiostatic (constant potential), potentiodynamic (cyclic voltammetry (CV) or pulsed potential), galvanostatic (constant current), galvanodynamic (pulsed current). The polymerization is usually carried out in a three-electrode configuration [28].

2.3.1. CV

An electrochemical technique where a potential is applied at the electrode, that is below the equilibrium potential of the reaction, potential is then increase linearly at constant rate to the to the maximum potential also called switching potential. After achieving the switching potential, the sweep is reversed to negative direction until the original potential value is reached. The sweep in the positive and negative direction is called anodic and cathodic scan respectively [29].

CV provides information about the oxidation potential of the CP monomer, film growth, redox behavior and surface concentration of the polymer by how much charge is being consumed [30]. An increasing peak current during anodic scan and formation of redox waves or nucleation loop before the oxidation potential are characteristics of polymerization and film deposition. In the first cycle a nucleation loop is being observed in which magnitude of charge during the cathodic scan is higher than anodic scan [28].

2.3.2. Potentiostatic polymerization

A constant potential is preferred method for electrodeposition of CPs whose overoxidation potential is very close to its oxidation potentials. An initial current drop is typically observed which is described as the oxidative electroadsorption of monomer and substrate passivation, following these process is the slow rise in current to maximum value and gradual decrease in current again [28].

2.3.3. Galvanostatic and galvanodynamic polymerization

A constant current is the most convenient for controlling the polymer thickness because it is proportional to the total charge passed. However galvanostatic deposition, includes mixed oxidation mechansims, poorer morphology, conductivity and general quality [28] [31]. On the other hand, pulsed current can achieve shorter chain length and/or higher degree of

conjugation. A long off-time helps the chain to fully oxidized before the next current pulse [28]. Pulsed current also enable rapid migration of dopant into PEDOT film [32].

2.3.4. In-situ polymerization

One of the most important electrochemical characterization techniques to gain information about chemical and electrical behaviour of conducting polymer is the in-situ electrochemical-conductance method. This enables us to monitor change in conductivity between the IDE while it is still in the polymerization solution [33].One way to perform in-situ electrochemical-conductance determination is with two independent potentiostats. One potentiostat (P1) delivers the needed electrical signal for polymerization (pulsed or linear sweep) also known as faradaic current (i_f)and the other potentiostat (P2) maintains the small constant potential between the IDE pad, known as drain potential (V_d), which in turn monitor the current (i_d) across the deposited conducting polymer layer which is analogous to the common transistor configuration as illustrated in Figure 6.

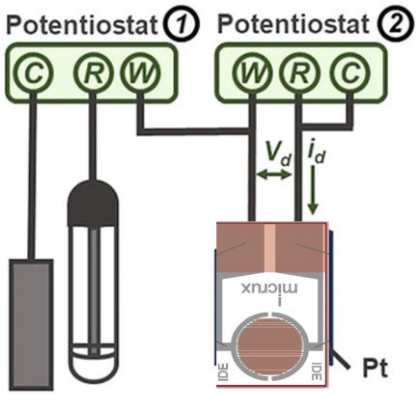

Figure 6. In-situ electrochemical-conductance measurement using two independent potentiostats. C=Counter Electrode (Pt-Rod), R=Reference Electrode (Ag/AgCl), W=Working Electrode (IDE). Ref [33] and Ref. [18]

2.4. **Conducting polymer as chemiresistive gas sensor**

Metal oxide chemiresistors are already commercially available and are used for industrial and environmental air quality monitoring [34]. They have great sensitivity, fast response time, low-cost manufacturability, good accuracy and stability [35]. However, these sensors need high operating temperature which raises power consumption [22].

Conducting polymer based chemiresistors which includes polypyrrole (PPy), PANI and PEDOT are suitable as sensing material for different gases. Its main advantage as chemiresistor

material over metal oxide is its room-temperature operation. However, conducting polymer based chemiresistors have generally lower sensitivity and poor selectivity compared to metal oxide based chemiresistors [14].

2.4.1. Gas sensing mechanism of conducting polymer

Gas conduction mechanism of conducting polymer can be explained by intra- and inter-chain transport. In intra-chain transport is localized and occurs along unidirectional pristine conjugated backbone at fast rates. Charge carriers consists of polarons, bipolarons and solitons where lowest unoccupied molecular orbital and highest occupied molecular orbitals of the conjugated backbone are involved. Photons and chemical dopants can influence these charge carriers. On the other hand, inter-chain charge transport is dependent on tunnelling or hopping of these charge carriers [14].

For p-type sensing material, oxygen is initially chemically adsorbed on the surface, which causes removal of electron from the conduction band which in turn causes increased in the hole concentration, when p-type material is exposed to an electron donating substance, for example ammonia, electrons are donated to the conduction band increasing the electron concentration as a result increases the resistance. On the other hand when exposed to electron withdrawing substance such as nitrogen dioxide, the electrons are withdrawn from the valence band, which increases the hole concentration therefore decrease in resistance [14].

2.4.2. Dopant

Chemical and physical properties of CPs can be alter using dopants. Doping level and property of dopant play a role in responses and conductivity of CPs. Small inorganic ions and acrylic dope PANI give different response to ammonia. meanwhile PPy doped with chlorate has higher conductivity than p-toluenesulfonate doped PPy. Another example is camphosuphonic acid doped PANI that has higher response in comparison with dipenyl phosphate and maleic doped PANI in detection of water vapor [20].

2.4.3. Performance characteristics

2.4.3.1. Sensor response

Response (R) is defined as the ratio between the sensor's resistance in the presence of the analyte gas (R_g) to the sensor's resistance to the baseline gas, which is commonly air (R_a). It can be R_g/R_a or R_a/R_g depending on the nature of both the sensor and the analyte gas and is summarized in Table 1 13].

Table 1. Evaluation of sensor response in the presence of reducing and oxidizing analyte. Adapted from [14]

Analyte	**n-type sensor**	**p-type sensor**
Reducing analyte (e.g., NH_3, NH_4, Acetone, Ethanol)	R_a/R_g R_g decreases	R_g/R_a R_g increases
Oxidizing analyte (e.g. NOx, CO_2, SO_2, O_2, O_3)	R_g/R_a R_g increases	R_a/R_g R_g decreases

R can be also calculated using Equation 1, in which its value gives symmetrical value of positive and negative for two types of sensor (n and p-type).

$$R = \frac{(R_g - R_a)}{R_a} \qquad \textit{Equation 1}$$

2.4.3.2. Response and recovery time

Response time (t_{RESP}) is defined as the time it takes for the sensor signal to reach 90% of the maximum signal change in the presence of the analyte gas. Recovery time (t_{REC}) is the time it takes for 90% of the steady-state signal to return to the baseline signal in the absence of the analyte gas [14]. Illustration of t_{RESP} and t_{REC} during the gas exposure were shown in Figure 7.

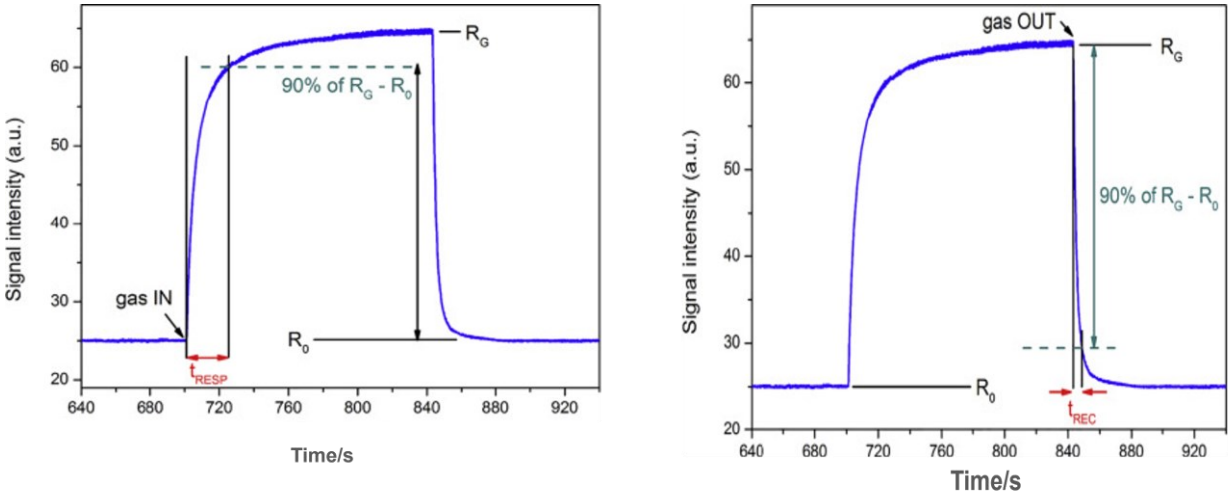

Figure 7. Left: Response time (t_{RESP}) illustration; Right: Recovery time (t_{REC}) illustration. R_g-resistance of the sensor upon exposure to analyte gas; R_0-resistance of sensor upon exposure to the baseline gas usually air

2.4.3.3. Sensitivity

Sensitivity is defined as the slope of calibration curve of gas response as function of gas concentration [36].

2.4.3.4. LOD

Many applications of gas sensors require detection at very low concentration. Therefore a concentration at which it is distinguishable from blank response is needed to determine. This concentration is called limit of detection and is calculated using Equation 2 [36].

$$LOD = \frac{3\sigma}{S}$$

Equation 2

σ- standard deviation of blank response

S- slope of the calibration curve

2.5. **Ionic liquid**

Ionic liquids are organic salts which exist as a liquid at room temperature. Such property makes it ideal property for chemical synthesis because it can act as both solvent and electrolyte. Another important advantages of using ionic liquids are their low vapor pressure. Some consider them as green solvents. They are soluble in different organic media, highly polar, have large electrochemical window and are easily recycled [37]. It has been found that ionic liquid

as medium for polymerization of conducting polymer such as polypyrrole results in altered film morphology and increased redox cycling stability[38].

2.6. **Percolation theory**

Percolation theory is a mathematical model used to describe a system wherein an atom, chemical bond or even grains have been connected to each other within a network structure to form a large but fragile cluster in which this connectivity has some consequence on the property of the whole system. It is the standard model to describe phase transition between the insulating phase to the conducting phase of a random network [39].

We can imagine a square lattice wherein certain fraction of squares are filled in a random manner with black square marks and other squares are empty, a cluster is defined as a group of neighboring dots (encircled in Figure 8). Percolation theory deals with this cluster formation. Sites are occupied with probability p. For finite lattice when the p is small there's only small chance of connected cluster or cluster percolating between boundaries. For p approaching 1, we are almost certain there's a cluster percolating through the system. Percolation threshold p_c is defined as probability p where an infinite cluster appears for the first time in an infinite lattice [40,41].

In the context of polymer chemistry, an electric DC current can only flow between connected clusters of conducting polymer chain, this current passess across to a unit voltage is called conductance. The change in conductance is greater in the percolation region than in the thin film region, Figure 8 shows an idealized graph of conductance as a function of polymer growth. For low polymer amount, theirs is no conductance because of insufficiently connected polymer chains. As more polymer is deposited, the system is approaching percolation region. When percolation threshold is reached there's non-linear relationship between amount of deposited polymer and conductance. Thin-film region on the other is reached when the conductivity of the system is dependent on film thickness [15,40].

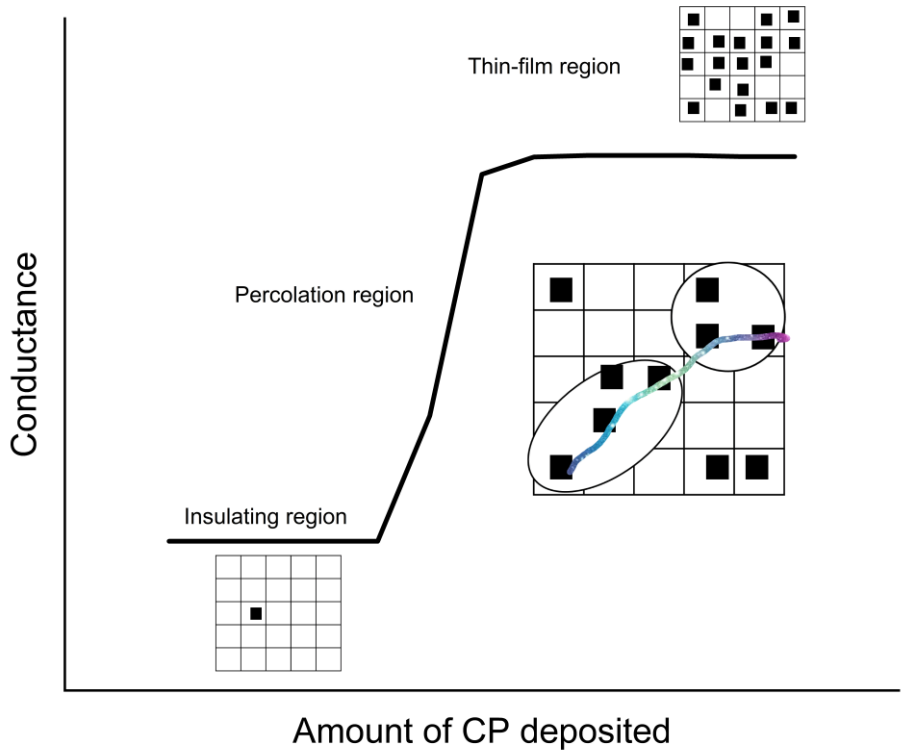

Figure 8. Ideal behavior of conducting polymer electrodeposition between two electrodes around the percolation threshold. Adapted from [15,40].

2.6.1 Explosive percolation (EP) theory

Explosive percolation is a variant of classical percolation, where there is a sharp percolation transition because of the delay in the emergence of spanning cluster. By allowing the system to form more smaller clusters than the larger ones, the formation of expansive component is prolonged. This phenomena in the formation of CPs were first reported by Robiños et. al wherein a polymerization in a stepwise continuous manner would promote EP growth [17,42].

2.7. **Electronic nose (EN) System**

Electronic nose is a system that mimic mammalian olfactory system, consisting of odour handling and delivery system, sensor array, electronic hardware for signal acquisition and processing and pattern recognition and classification algorithms.

2.7.1. Gas handling and delivery set-up

Main types of vapor handling are sample flow system and static system. Large number of samples can be analyzed in the flow system, wherein sensors are placed in a vapour flow which in turns allow rapid exchange of vapor. On the other hand, static system does not use vapor flow instead, it waits for a steady-state response of the sensor exposed to constant vapor concentration. Both set-ups are closed system [43].Most of the sample vapor are generated from evaporation of liquid samples. When there is a mixture of compounds in the sample, the partial pressure of the compound in the vapor (P_A) is proportional to the product of mole fraction of the compound in the solution (X_A) and the vapor pressure of the pure compound (P_A^0) (see Equation 3).

$$P_A = X_A \times P_A^0 \qquad \textit{Equation 3}$$

2.7.1.1. Bubbler

An example of flow system is a bubler, wherein the vapor is created through bubbling, and carrier gas takes it away. Although a relatively easy method of obtaining vapor, liquid samples can be carried directly to the sensor due to heavy bubbling [27]. Bubbler set up is illustrated in Figure 9.

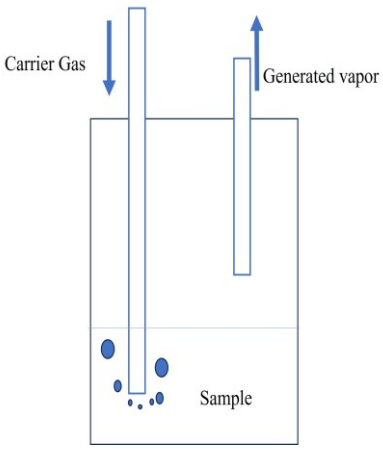

Figure 9. An illustration of bubbler set-up, an example of a sample flow system.

2.7.1.2. Static system

Steady-state response of a sensor to the vapor is being measured in a static system. In a closed chamber containing a volume of liquid sample is being evaporated and the vapour envelopes the sensor. The principle is illustrated in

Figure *10***.**

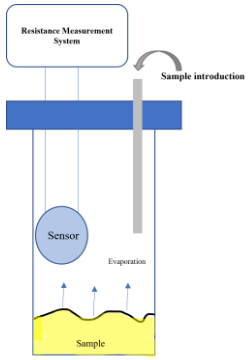

Figure 10. Principle of static system for vapor delivery to chemiresistor.

2.7.2. Sensor array

A chemical sensor array is collection of sensing components that produce quantifiable outputs from chemical interactions of each component. Chemical sensors which is the core of an EN system can be, inorganic (metal oxides), organic and polymer materials (CP). Sensor array can be identical or dissimilar. Identical sensor array enhances the precision of the signal while dissimilar sensor array is needed for cross-verification [44].One important aspect of EN system is the number of sensors in the array, which is highly dependent on the sample composition. If the sample consist of a mixture of gases or if the gas concentration changes the large number sensors are desirable to minimize uncertainty. If samples are pure compounds the one or two sensors are enough [44].

2.7.3. Data acquisition and processing

The feature extraction method is one of the important aspects of improving performance of EN systems because no matter what pattern recognition method is selected the sample distribution in the feature space has strong relation to recognition rate. The aim of feature selection is extracting maximum information with less redundancy, which can represent a fingerprint of the gas sample. Features can be extracted from original response curves, commonly from steady-state and transient responses (see Table 2) [45].

Table 2. List of commonly use feature extraction method from the original response curves of sensors [45].

Feature	**Description**
Maximum value	a. Difference $X_{ij} = R_{max} - R_{min}$ b. Relative difference $X_{ij} = R_{max}/R_{min}$
Time of special responses	Time where a special response appeared
Area	Area under the sensor response curve and time axis
Derivative	$D' = \frac{dx}{dT}$
Second derivative	$D' = \frac{d^2x}{dT^2}$

2.7.4. Pattern recognition and classification (PARC)

Multivariate data obtained from chemical sensor array can be processed through variety of techniques or algorithms. They are generally divided into supervised and unsupervised learning. In a supervised learning, odors are delivered to the EN and based on known descriptor of the odor and its feature it will be held in a knowledge base. The learnt relationship will be used to predict the membership of the unknown odors. Meanwhile unsupervised learning is used to discriminate the odor and its features without the prior knowledge of its descriptor or class [43].

2.7.4.1. Linear Discriminant analysis (LDA)

LDA one of the most common supervised methods of learning, in which it reduces the dimensionality of the data set by defining new variables called the discriminant functions (DFs) and used other criteria to construct them as linear combinations of the original variables. LDA maximizes the distances between the centroids of classes (between-class variance) and minimizes the within-class variance. This method enhances the separation between classes of each samples [46].

3. Experimental Section

3.1. **Materials**

Platinum and Gold IDEs on glass substrate consisting of 180 pairs of 5 µm wide fingers and 5 µm finger gaps (Micrux, Spain) as illustrated in Figure 11 were used. New IDEs were used for each experiment.

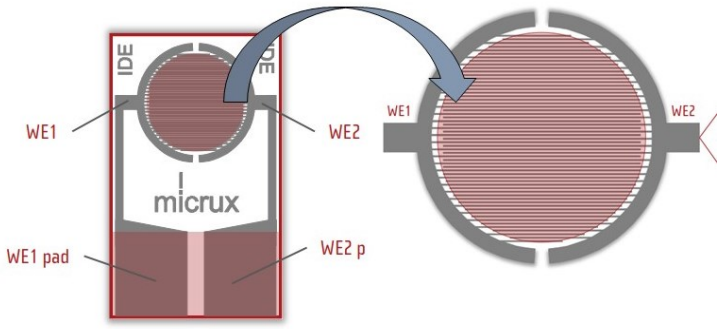

Figure 11. An illustration of the IDE and gaps between each fingers. Dimension: 10x6x0.75 mm. WE (Working electrode). Adapted from [48].

Used monomers were 3,4-ethylenedioxythiophene (EDOT, $C_6H_6O_2S$, ≥97%, Sigma Aldrich) and aniline ($C_6H_5NH_2$, 99%, Sigma Aldrich). The solvent was acetonitrile (MeCN, C_2H_3N anhydrous, 99.8%, Sigma Aldrich). Tetrabutylammonium perchlorate ($TBAClO_4$, $N(C_4H_9)_4ClO_4$, ≥99.0%, Sigma Aldrich) was used. Ionic liquids: 1-butyl-3-methylimidazolium hexafluorophosphate ($BMIMPF_6$, 99%) and 1-ethyl-3-methylimidazolium bis(trifluoromethylsulfonyl)imide (EMIMFSI 99%) were purchased from IOLITEC GmbH and were used as received. Additional chemicals includes ethylene glycol ($HOCH_2CH_2OH$, 99 %, Fluka), sulfuric acid (H_2SO_4 ≥95%,), ammonia solution (NH3, 25%).

3.2. **Electropolymerization**

Ivium CompactStat.h and Ivium-n-stat (Ivium Technology) were used as a potentiostat/galvanostat system. Ag/AgCl reference element was made by oxidation Ag wire (1 *d* x 50 *l* mm) in 3 M KCl aqueous solution applying 20 mA for 10 min using Metrohm AG Coulometer Type 211. Ag/AgCl was used as a pseudo-reference electrode (RE). Platinum rod (3.1 *d* x 49.7 *l* mm) was used as the counter electrode (CE). The two pads of the IDEs were

connected via single alligator clips and served as a working electrode (WE). Glass cell was manufacture by Princeton Applied Research.

Every electropolymerization was conducted in a 30 mL glass vessel with 15 mL of polymerization solution and with the custom-made PTFE lid. A nitrogen gas was used to purge the solvent from dissolved oxygen for 10 min for both acetonitrile and ionic liquids and then was used as gas blanket above the solution. Only the circular region of the IDEs was exposed to the solution as illustrated in Figure 12.

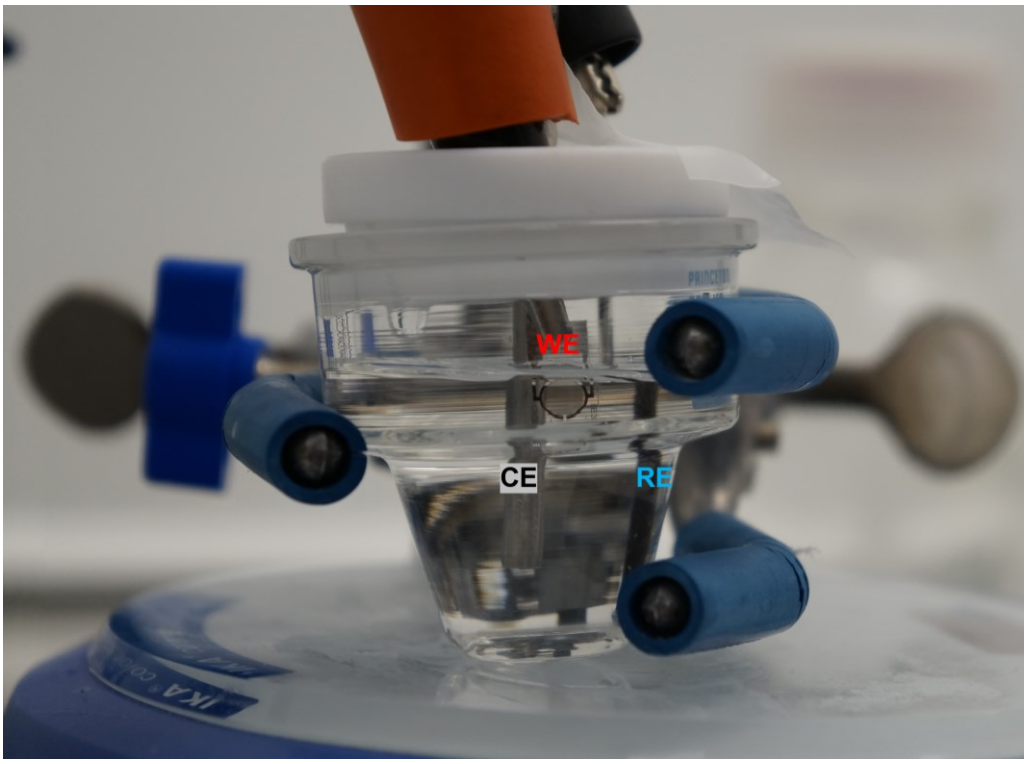

Figure 12. The three-electrode set up used in the electropolymerization experiments. ***WE****: IDE;* ***RE:*** *Ag/AgCl;* ***CE:*** *Platinum Rod.*

3.2.1. Preparation of polymerization solution

3.2.1.1. PEDOT

0.01 M EDOT monomer was prepared for the electrochemical synthesis of the conducting polymer. Solvents were either acetonitrile or ionic liquids ($BMIMPF_6$ and EMIMFSI). For electropolymerization involving acetonitrile 0.1 M of $TBAClO_4$ served as a supporting electrolyte and dopant. Ionic liquid served both as a solvent and as a dopant.

3.2.1.2. PANI

0.05 M of monomer aniline was prepared in 0.5 M sulfuric acid (dopant) for electropolymerization of PANI.

3.2.2. Determination of electropolymerization potential (E_{EP})

Cyclic voltammograms were obtained to determine the oxidation potential (E_{EP}) of the monomer and to monitor the electrochemical behavior of the system during oxidation and reduction process. A scan rate of 100 mV/s was applied from -1.0 to 1.5 V vs Ag/AgCl in the three-electrode system. A potential near the nucleation loop was chosen as E_{EP}.

3.2.3. Potenstiostatic polymerization

After determination of the E_{EP}, this DC potential was applied to the fresh IDE for 60 s and then IDE was taken out of the solution, rinsed with acetonitrile, and dried in the air. Resistance between pads was then measured by applying a DC potential of 1.0 V for 60 s to both pads. Following Ohm's law, conductance was then determined. Conductance vs transient time graph was constructed to monitor the IDE is in insulating, percolation, and thin film regions. Additionally, cumulative charge needed to reach the thin film region was also determined.

3.2.4. Galvanostatic polymerization

The potentiostatic polymerization revealed the ideal cumulative charge needed to reach the percolation region. The charge was partitioned into five rounds so that after the 5th round the IDE should be in percolation region. Each round consisted of applying certain electropolymerization charge called Q_{EP}, taking out the IDE from the solution, rinsing with MeCN and drying it out in the air.

3.2.5. Explosive percolation

Method developed by Robinos et. al was employed and will in this document be referred to as as Explosive Percolation (EP) method [17]. It is described as stepwise discontinuous galvanostatic polymerization.

3.2.6. Pulsed galvanostastic polymerization

To improve the repeatability of the electropolymerization process while maintaining the stepwise discontinuous galvanostatic electropolymerization, a pulsed galvanostatic polymerization was applied. With IDE in the in the polymerization solution, a short pulsed of

Q_{EP} was applied and after that the system was set to an “Open cell” for certain period of time. After polymerization the IDEs were wash with acetonitrile and dried in air.

3.2.7. In-situ conductance monitoring

PEDOT was electropolymerized via chronoamperometry by applying voltage on P1 (i_f) while maintaining small voltage at P2 to measure the conductance between pads of IDEs as described by Castell et. al [18] and illustrated in section 2.3.4. After polymerization the IDEs were washed with acetonitrile and dried in the air.

3.3. **Effect of electrochemical p-doping**

Robiños et al. claimed that by applying a small oxidation potential to the polymer the performance of the sensor would increase. The claim was tested by comparing the sensor conductance and its response before and after the electrochemical conditioning. For both cases of PEDOT and PANI this was accomplished by applying 0.1 V between two pads of the IDE for 60 seconds in the monomer-less polymerization solution.

3.4. **Characterization of sensor**

Static odor handling set up (see Figure 13) was made by, puncturing a hole through a vial cap and putting the Micrux IDE cable connector which consist of two contact wires connected to the pads of IDE. A potentiostat in 2-cell configuration was connected to the cable leads to monitor the resistance of IDE. Varying concentration of model gas (ammonia) was made in 30-ml vial by diluting concentrated ammonia (ca. 25 %) with ethylene glycol. Following Raoult’s law, the mole fraction of ammonia in the solution should be proportional to ammonia vapor partial pressure.

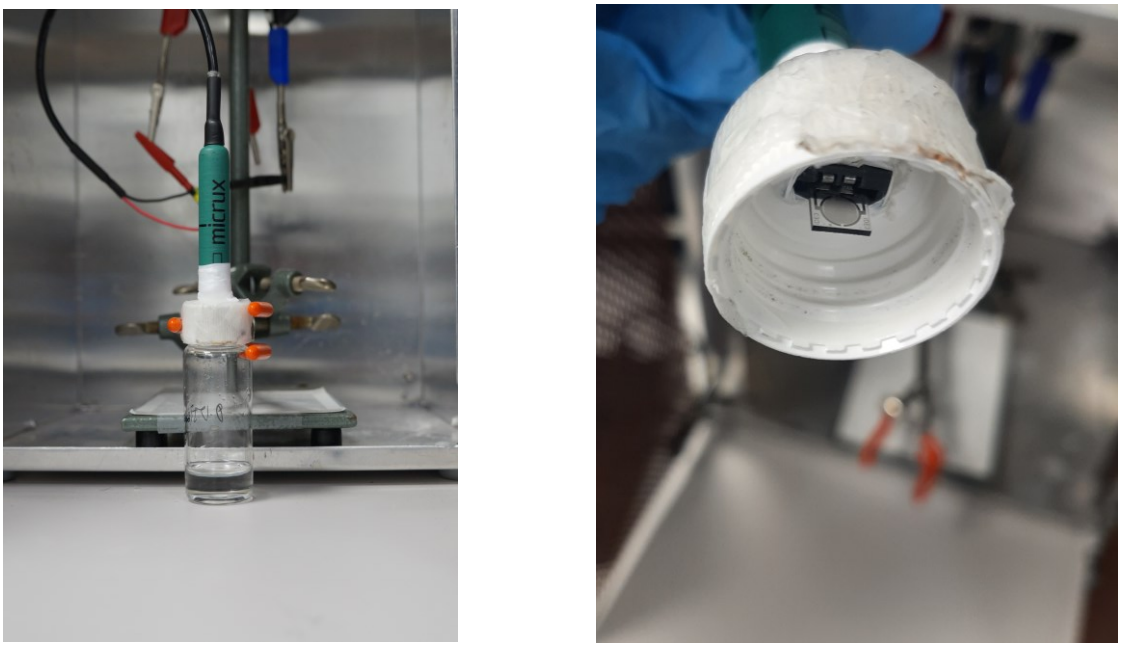

Figure 13. A custom-made static odor handling set up.

3.5. **Electronic nose (EN) system**

A sketch and actual realization of gas chamber that was used for electronic nose experiments are presented in Figure 14 and Figure 15. The chamber was fabricated in Åbo Akademi workshop and made up of two circular steel plates, with 8 slots for IDEs on the bottom plate. An o-ring was sandwiched between plates to make it air-tight. On the upper plate there are air-tight inlet and outlet to let the gas flow in and out of the chamber. The chamber was tightened with 8 screws.

The eight IDEs were connected to eight Ivium potentiostat (Q91300, Q91301, Q91302, Q91303, D41224, D41225, B40511, b12705) in 2-cell configuration in which a 1.0 V potential was applied (see Figure 16) to monitor changes in resistance between pads of IDE. Syncing channels was enabled in *IviumSoft* software for simultaneous resistance monitoring.

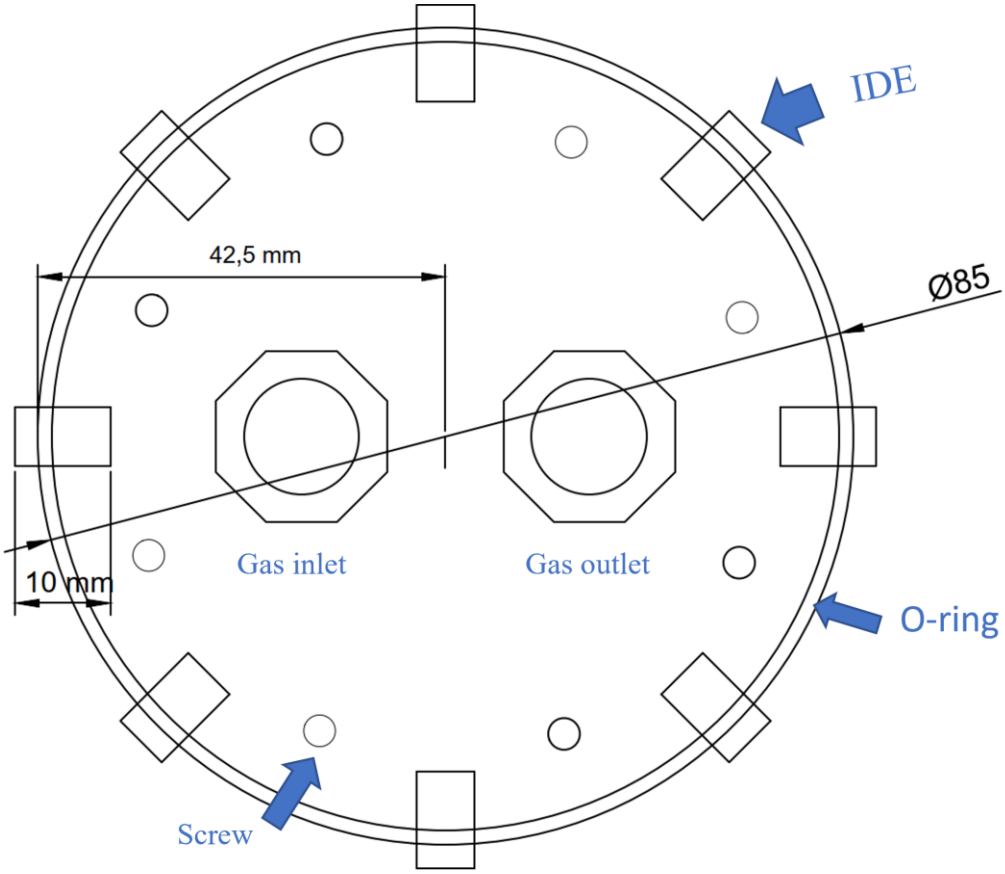

Figure 14. A diagram of flow-through gas chamber. Gas flows through an inlet and exits at an outlet in the process exposing the IDEs to the gas which is tightened by aluminum screws.

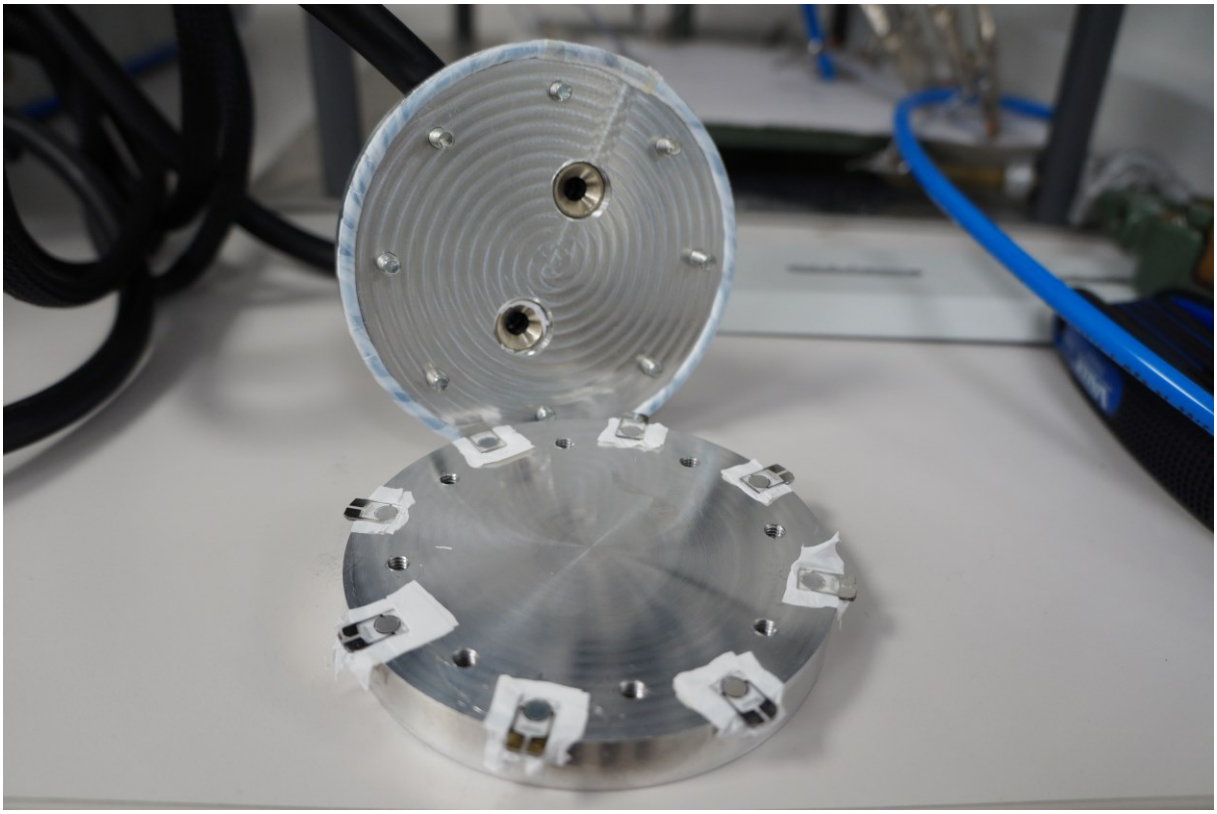

Figure 15. Arrangement of IDEs in the gas chamber

Figure 16. Actual set-up of gas chamber showing how gas flows.

To generate solvent's vapor, the 20 ml crimp vial was filled with 5 mL aliquot and sealed with crimp caps via crimper. The air pump (Claypower LP27-12) was to set 3.1 V to generate 0.39 L/min flow of air. The air travel through the vial generating bubbles and transporting the vapor to the gas chamber. After exposing the IDE to the vapor for 30 s the system was purged for 180 s by replacing the vial with an empty one. Before any measurement of the next sample the system was purged again for 30 s.

3.6. **Feature extraction and classification algorithm**

Maximum value was obtained from raw data by taking the average resistance between 10-30 s (air, R_a) and dividing it by the average resistance between 50-70 s (sample, R_g) for sensors that behaved like n-type materials. For p-type sensors the numerator and denominator were reversed.

The dataset containing solvent name and the maximum value of each sensor were given "*SolventData*" filename. Linear discrimant analysis algorithm was used to create a model to classify solvent samples. Matlab R2021b was used to perform LDA.

4. Results and Discussion

4.1. **Potentiodynamic polymerization**

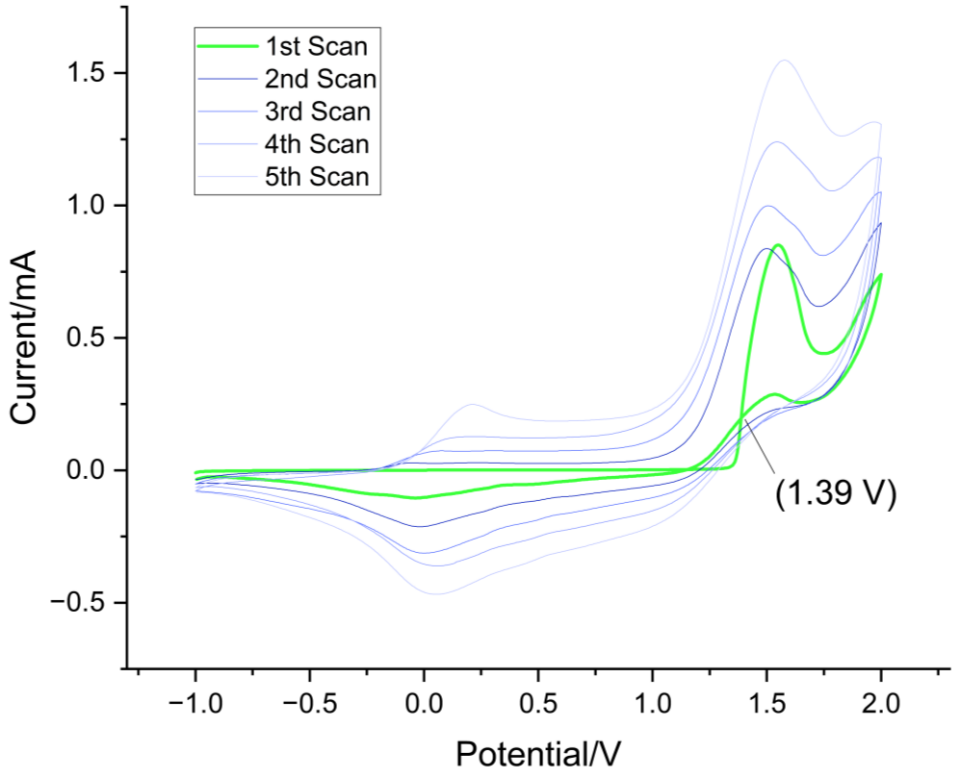

Figure 17. Potentiodynamic Polymerization EDOT in 0.01 M MeCN/0.1 M TBAClO4; RE: Ag/AgCl; WE: IDE; CE: Pt Rod, Scan rate: 0.1 V/s.

A CV was performed from -1.0 V to +2.0 V and back to -1.0 V to determine the oxidation potential of EDOT in MeCN in the presence of $TBAClO_4$. An increase of anodic current was observed at 1.1 V, which corresponds to the beginning of oxidation of EDOT followed by formation of an anodic peak at 1.3 V as illustrated in Figure 17**.** This phenomenon is consistent and close to the values reported by Melato et al. [49].

Four (4) subsequent scans showed a steady increase of current, as shown in Figure 17**,** which indicated growth of the polymer.

4.2. **Potentiostatic polymerization**

Based on the CV results described in the previous paragraph a constant potential of 1.3 V was applied to the IDE for 1.0 seconds for five consecutive runs. After each run the IDE was washed with MeCN and dried. The conductance of IDE in the air was measured between pads of IDE. Alongside the cumulative charge was also monitored.

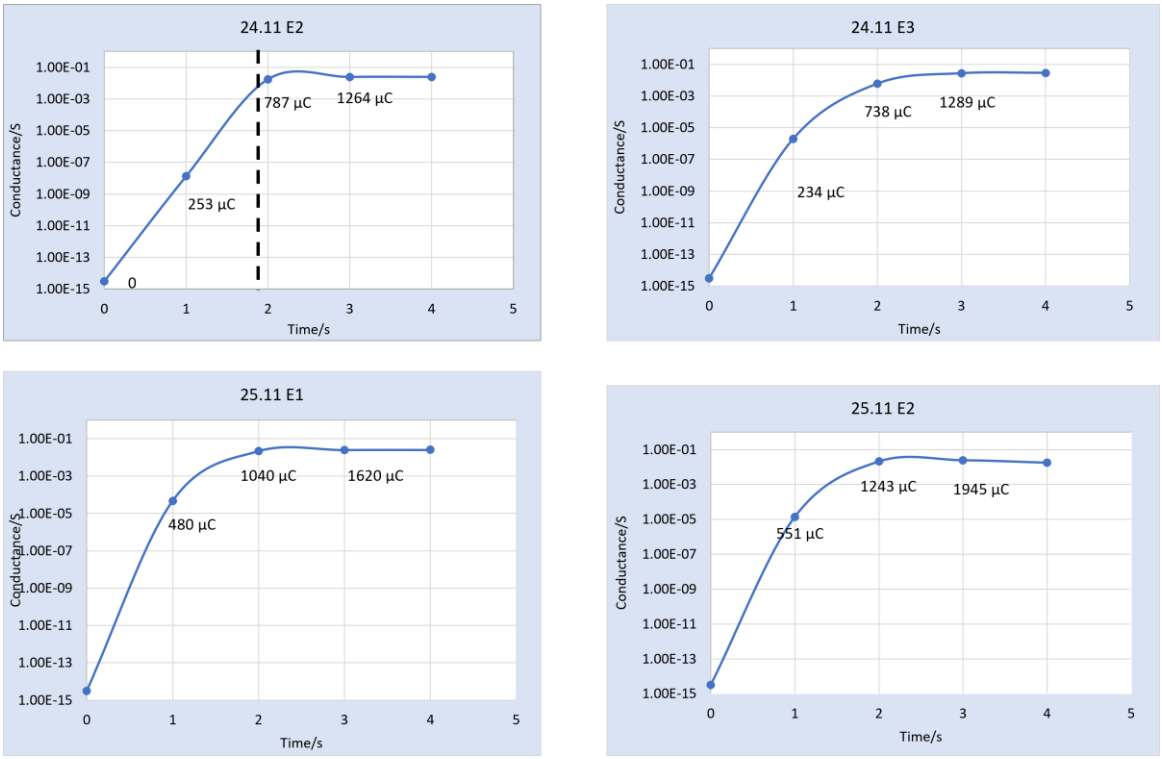

Figure 18. Potentiostatic polymerization of IDE; applied voltage: 1.3 V; time: 1.0 second. Dashed line separates percolation region from thin film

Potentiostatic polymerization with subsequent conductance monitoring reveals a sudden increase in conductance just after 2 cycles or seconds of applying constant potential. Just as described by percolation theory. Therefore we will refer to it as the percolation region. After the percolation region is the plateau of conductance which we will refer to as thin film region.

As shown in Figure 18, the percolation region starts after one to two cycles. However, the determined cumulative charge showed that the process is not so repeatable. Thin film region was reached between 787 µC to 1243 µC. This makes potentiostatic polymerization not an ideal way of producing percolation IDEs. Nevertheless, the provided information is an important parameter for producing percolation IDE as we will see later.

4.3. **Galvanostatic polymerization using EP Method**

One way of controlling the deposition of PEDOT is to control the amount of charge we apply to the system. In theory, this technique will be more reliable since a certain amount of charge also corresponds to a certain amount of monomer being oxidized or reduced.

The percolation region could end as early as 787 μC. We wanted to stop before that point to be sure we are in the percolation region. Therefore, a charge of 500 μC was set as the target. If we wanted to deliver that cumulative charge in 10 cycles, then we needed to apply 10 μA of current for 5 s per each cycle.

Consequently, each of the cycles involved applying 50 μC charge to the IDE in the electropolymerization solution, taking IDE out of the solution, washed it with MeCN and drying it in the air. Afterwards, conductance in the air was measured between pads of IDEs. This experiment was repeated several times for new IDEs and it is illustrated in Figure 19.

A distinction between insulating, percolation and thin film region was finally realized through galvanostatic polymerization. IDEs started as a non-conducting material but upon deposition of PEDOT between electrodes of IDE there was a sudden increase in conductance. However, the repeatability of the procedure was far from being perfect. The percolation region does not appear at the same moment in the polymerization process. IDE “05.12 E1” for instance had become conductive starting at 100 μC while IDE “1.12 E2” becomes conductive at 200 μC. Moreover, some IDEs have a very early thin film region.

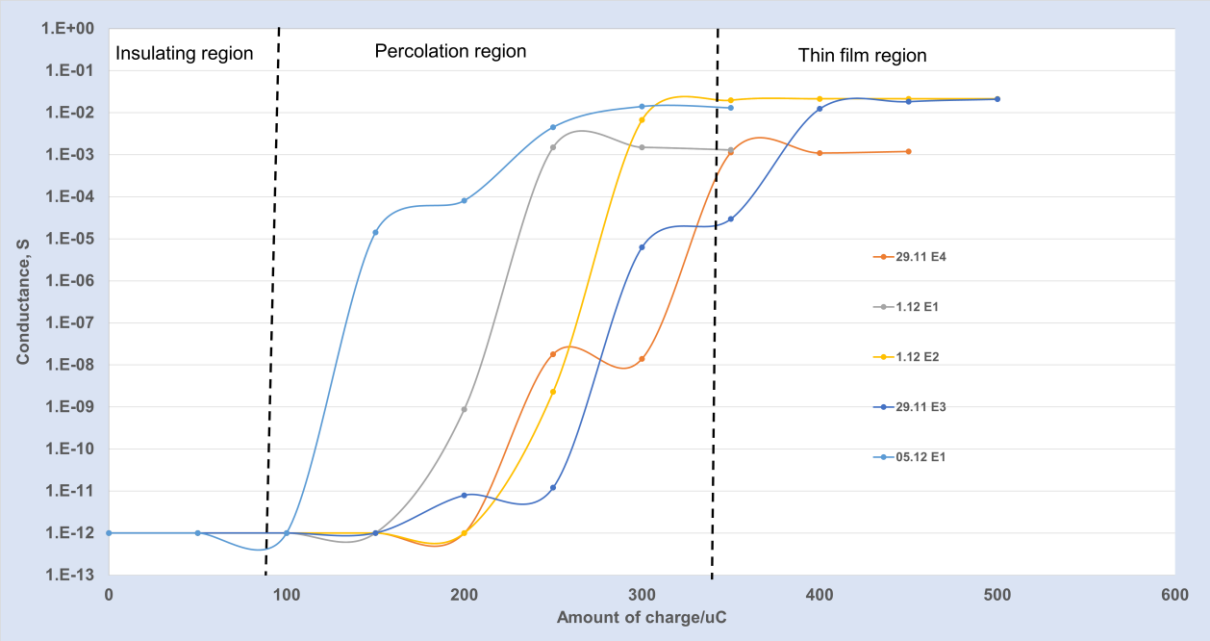

Figure 19. Percolation growth curve from stepwise galvanostatic polymerization of 0.01 M EDOT/0.1 M TBAClO4 in MeCN, WE: Pt IDE, RE: Ag/AgCl, CE: Pt Rod. Each curve was from different IDE while each point is measured conductance against air after each round.

4.4. **Pulsed galvanostatic polymerization**

Works of Robiños et al. demonstrated that stepwise discontinuous galvanostatic polymerization is crucial to the sensitivity of this conducting polymer based chemiresistor [17]. To simulate this stepwise process without taking out the IDE from the polymerization solution, the following process was employed. 10 µA of current was passed during 5 s followed by a rest period (0 µA) for 10 s. A five-fold repetition of this process resulted in a total of 250 µC charge delivered to the IDE. According to galvanostatic polymerization in Figure 19 this should lead us to the percolation region. Five sensors were made on the same day using pulsed galvanostatic polymerization and after that each initial conductance was tabulated in Table 3 and exposed to the model gas (NH_3).

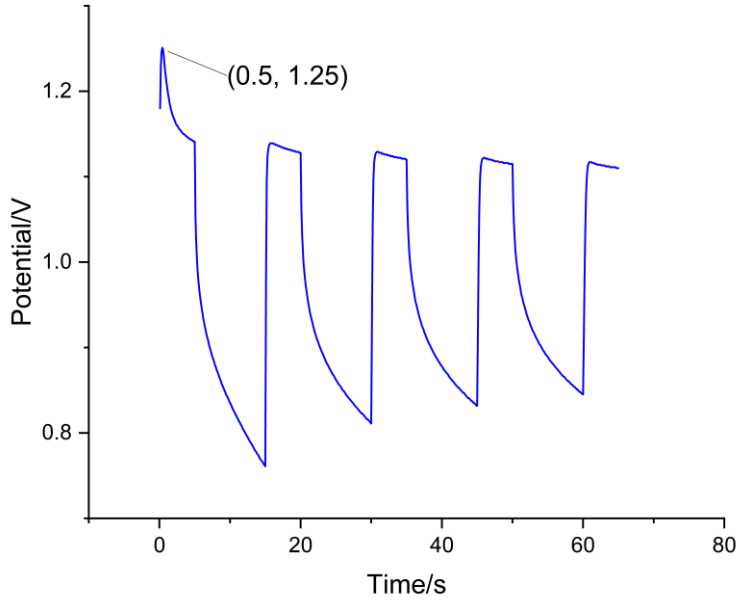

Figure 20. Chronopotentiogram of pulsed galvanostatic polymerization of 0.01 M EDOT/0.1 M TBAClO4 in MeCN, WE: Pt-10 IDE, RE: Ag/AgCl, CE: Pt Rod.

Table 3. Conductance of IDEs in the air after Pulsed Galvanostatic Polymerization. Irreversible- means no appreciable signal was obtained. LOD is expressed as the mole fraction of ammonia in the solution of ethylene glycol and conc. ammonia.

IDE	Initial Conductance, S	Ammonia sensing
Pt-10	7.80E-09	Reversible
Pt-11	3.96E-05	Irreversible
Pt-12	7.98E-07	Irreversible
Pt-13	2.84E-05	Irreversible
Pt-14	2.49E-08	Reversible

Chronopotentiogram of pulsed galvanostatic polymerization (see Figure 20) shows a peak potential at 1.25 V which in agreement with the oxidation potential shown in previous CVs and subsequent decreased in potential was shown as less energy is needed to add monomer to the growing oligomer.

The pulsed galvanostatic polymerization yielded IDEs with varying initial conductance (see Table 2) from 10^{-5} to 10^{-9} siemens even though all IDEs were manufactured on the same day and using the same polymerization conditions. However, based on Figure 19, all sensors manufactured in Table 3 fall under percolation region.

4.5. **n-type PEDOT**

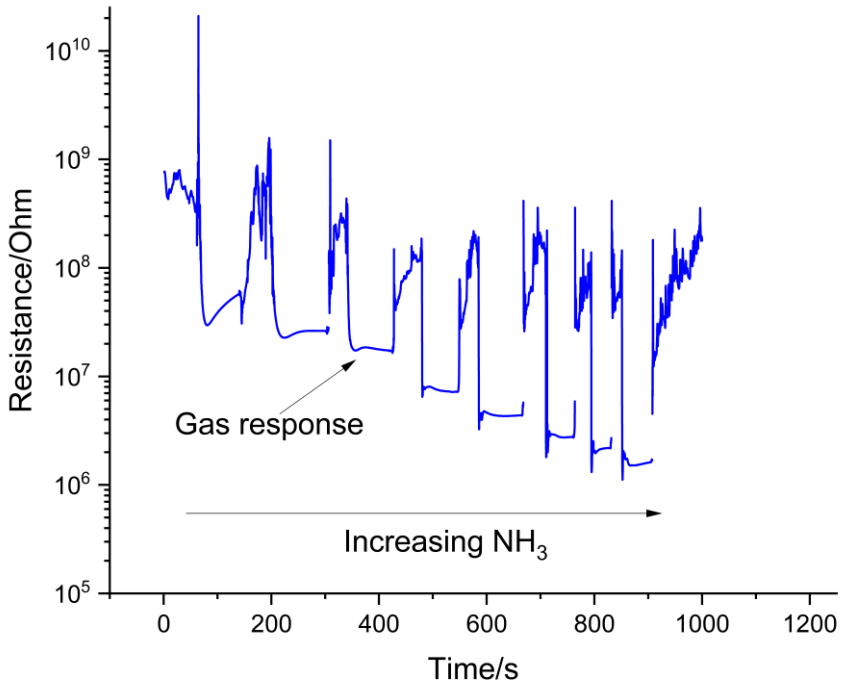

Figure 21. Raw sensing response to increasing NH_3 concentration of IDE: Pt-10.

Manufactured sensors were expose to varying concentrations of ammonia, IDEs: Pt-10 and Pt-14 were the only sensors that had reversible response (see Table 3), other sensors where don't have appreciable response towards ammonia.

Reversible sensors (Pt-10 and Pt-14) showed interesting behavior, they behaved as n-type material that is, the resistance decreases upon exposure to reducing gases such as ammonia (see Figure 21). Although this behavior of PEDOT percolation has been previously reported by Robiños et. al, such gas mechanism was accounted for by electrochemical conditioning i.e applying a small voltage to the polymer after polymerization or p-doping. Pt-10 and Pt-14 were able to exhibit reversible n-type behavior without electrochemical conditioning were able to exhibit reversible n-type behavior.

4.6. **Linearity and LOD of n-type PEDOT**

Pt-10 was exposed to both high level (Figure 22) and low level (Figure 23) of ammonia concentration. High dynamic range was observed, with interestingly increased sensitivity as concentration of ammonia increases (Table 4). Data from low level ammonia concentration was used to determine the LOD of both Pt-10 and Pt-14.

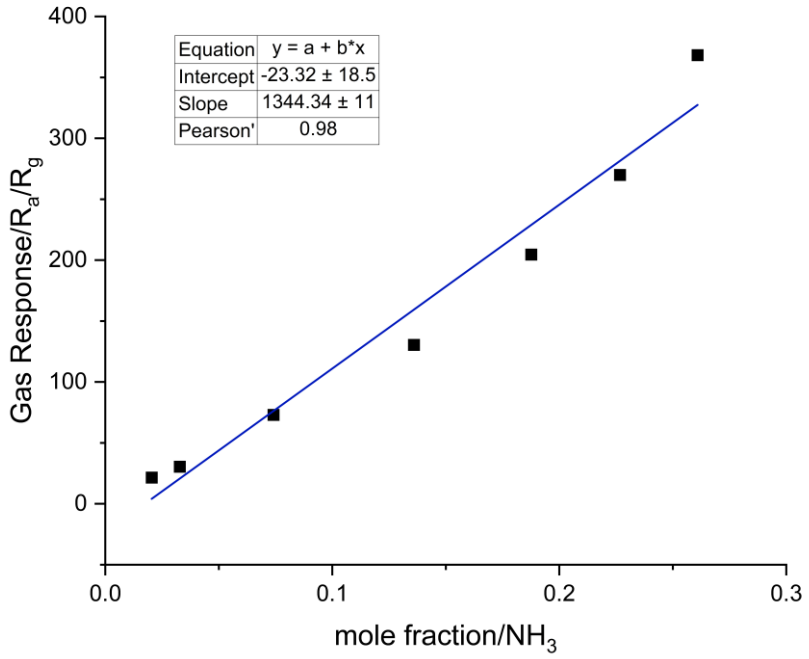

Figure 22. Calibration curve of response vs high ammonia concentration using static odor handling set-up. IDE: Pt-10

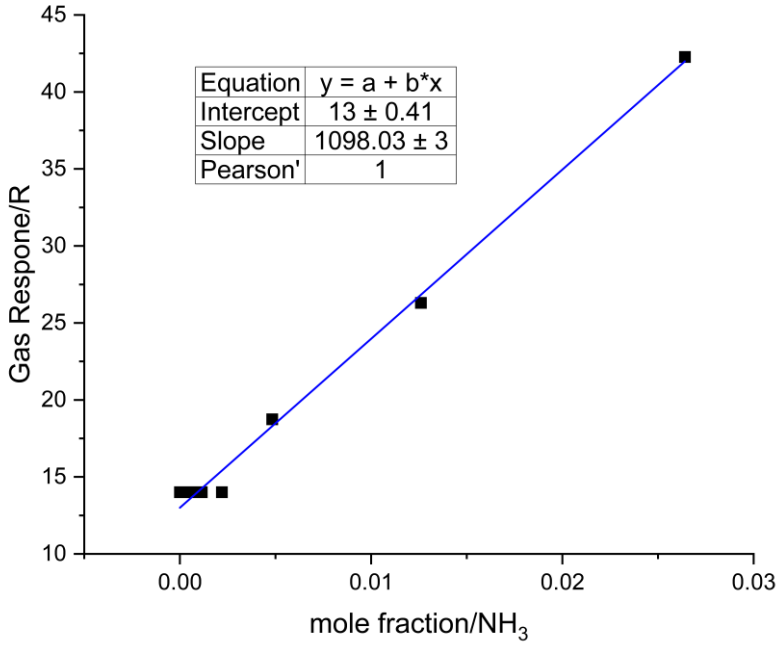

Figure 23. Calibration curve of response vs low ammonia concentration using static odor handling set-up. IDE: Pt-10

A calibration curve for low level concentration of ammonia was also constructed for Pt-14 (see Figure 24). Pt-14 exhibited greater sensitivity (around three times) and higher LOD towards ammonia compared to Pt-10 (see Table 4). This highlighted the non-repeatability of produced sensor not only in terms of initial conductance but also in terms of gas sensing performance.

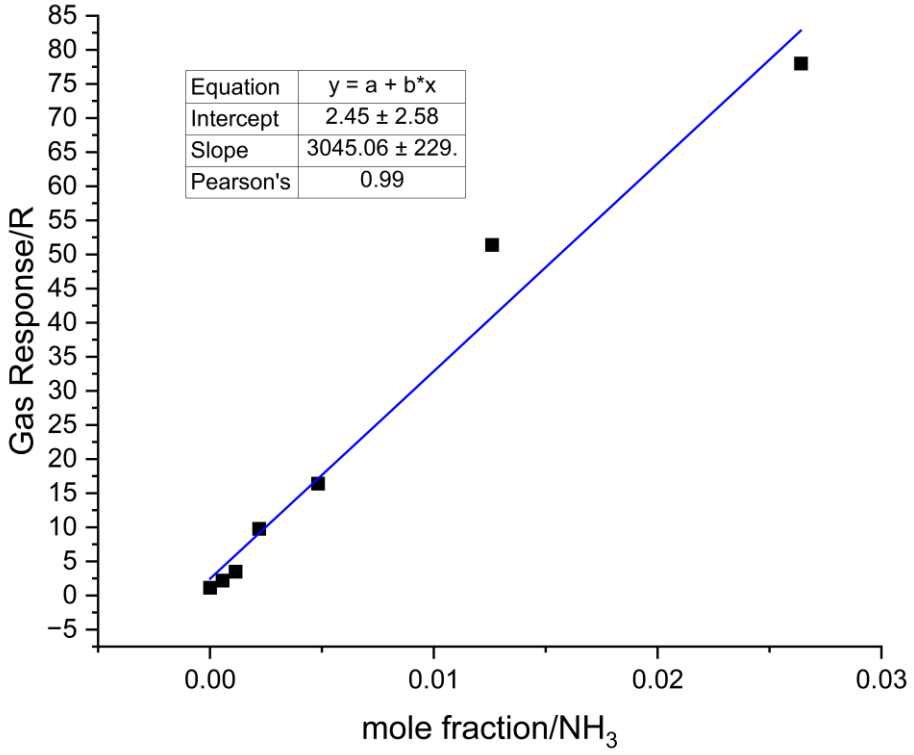

Figure 24. Calibration curve of response vs low concentration of ammonia using static odor handling set-up. IDE: Pt-14

Table 4. Sensitivity and LOD of n-type PEDOT sensor

IDE	**Sensitivity, R/mole fraction NH_3**	**LOD, mole fraction NH_3**
Pt-10 (High)	1344	2.8E-3
Pt-10 (Low)	1098	
Pt-14 (Low)	3045	1.2E-3

4.7. **Percolation growth curve in ionic liquid**

4.7.1. CV

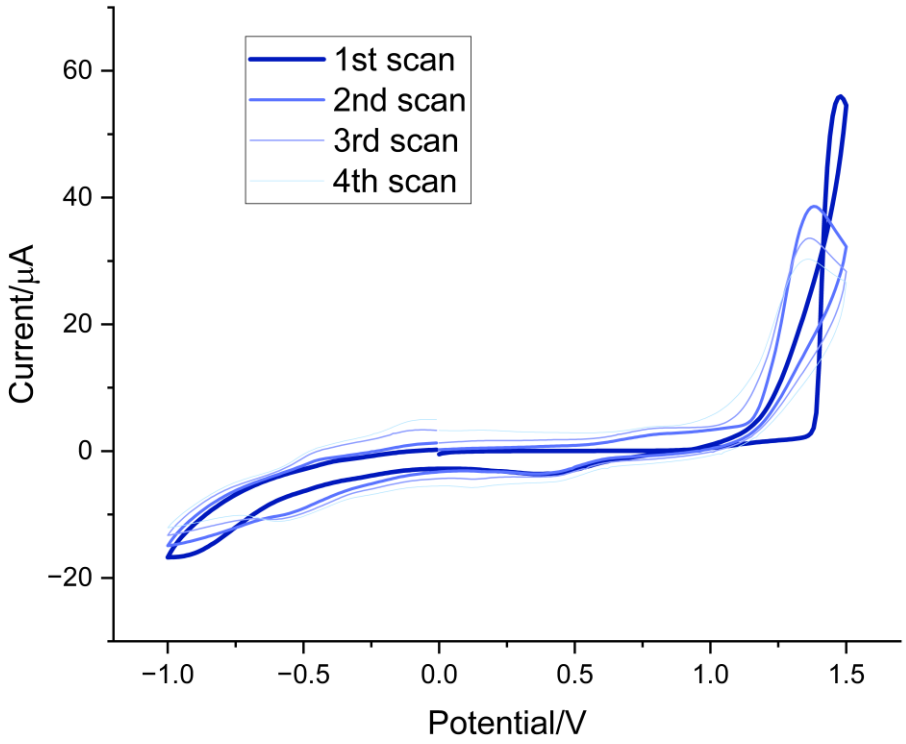

Figure 25. Potentiodynamic polymerization 0.01M EDOT in $BMIMPF_6$; RE: Ag/AgCl; WE: IDE; CE: Pt Rod, Scan rate: 0.1 V/s.

A nucleation loop (1st scan in Figure 25) was observed during the first scan however, no increase in current was observed in the succeeding scans. It maybe accounted for high viscosity of $BMIMPF_6$ (267 cP) compared to well know polymerization solvent like acetonitrile (0.38 cP). According to Walsh et. Al, viscosity plays important role in mass transfer in iodide/triodide redox system of imidazolium-based ionic liquids and high viscosity of ionic liquid leads to slow rate of mass transfer in voltammetry [50]. In our case, the formation of nucleation loop after increasing the scan rate temporarily compensated the viscous $BMIMFP_6$ however, subsequent scan resulted in mass transfer limited polymerization. Since EP method of polymerization involved stepwise discontinuous steps, diffusion related issues should not affect the polymerization of CPs.

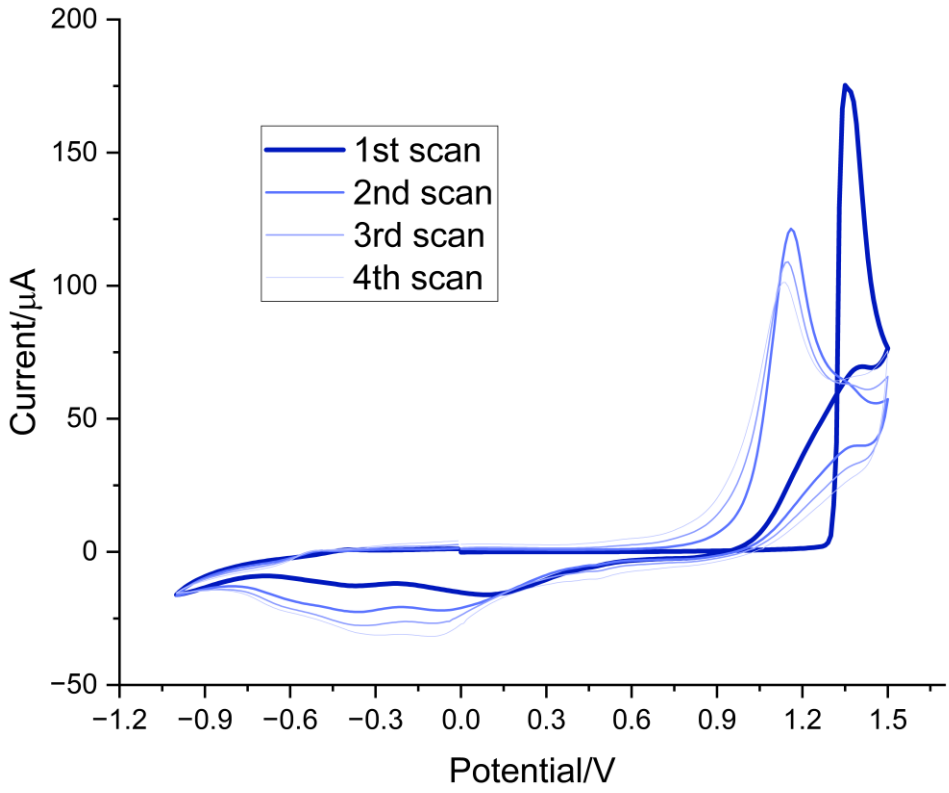

Figure 26. Potentiodynamic polymerization 0.01M EDOT in EMIMFSI; RE: Ag/AgCl; WE: IDE; CE: Pt Rod, Scan rate: 0.1 V/s.

Potentiodynamic polymerization of EDOT in EMIMFSI (see Figure 26) had similar profile however with higher current peaks and seemingly increasing oxidation potential per cycle.

4.7.2. Potentiostatic polymerization

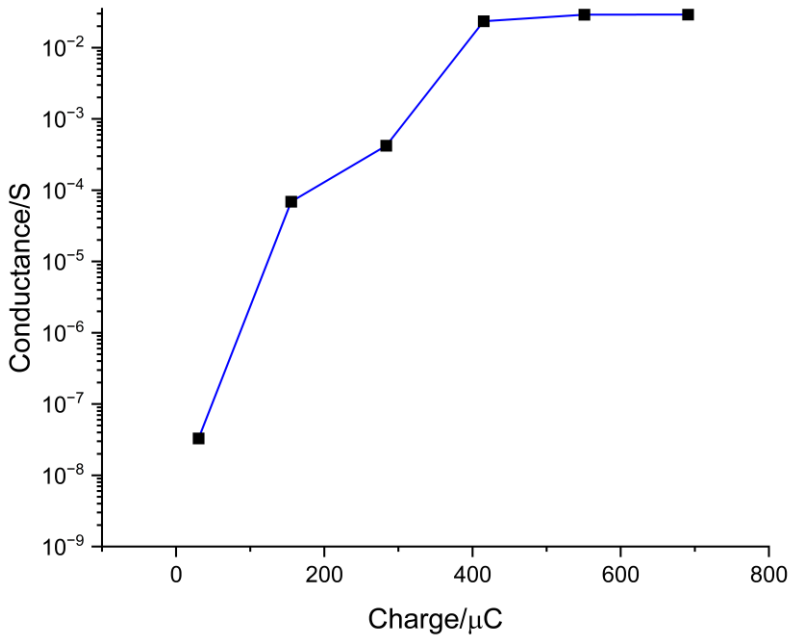

Figure 27. Potentiostatic polymerization of 0.01 M EDOT in EMIMFSI RE:Ag/AgCl; WE: IDE; CE: Pt Rod, E_{EP} = 1.3 V for 1 s.

Percolation growth curve of EDOT in EMIMFSI is presented in Figure 27, potential of 1.3 V as applied for 1 s and cummulative charge was determined. A total of 700 μC of charge was delivered to achieve thin-fim, the sensor produced was given an ID of **Pt-62**.

4.7.3. EP polymerization

Based on CV experiment (see Figure 25) the polymerization of EDOT in $BMIMFP_6$ occurs within current of 20-60 μA, therefore 20 μA current was chosen to deliver charge (Q_{EP}=100 μC) during 5 seconds. Each round consisted of delivering the Q_{EP} to the IDEs while in polymerization solution of 0.01M EDOT and $BMIMFP_6$ under nitrogen blanket. After each round IDEs were taken out of solution washed with ethanol and dried in the air. Conductance in air vs amount of charge is presented in Figure 28.

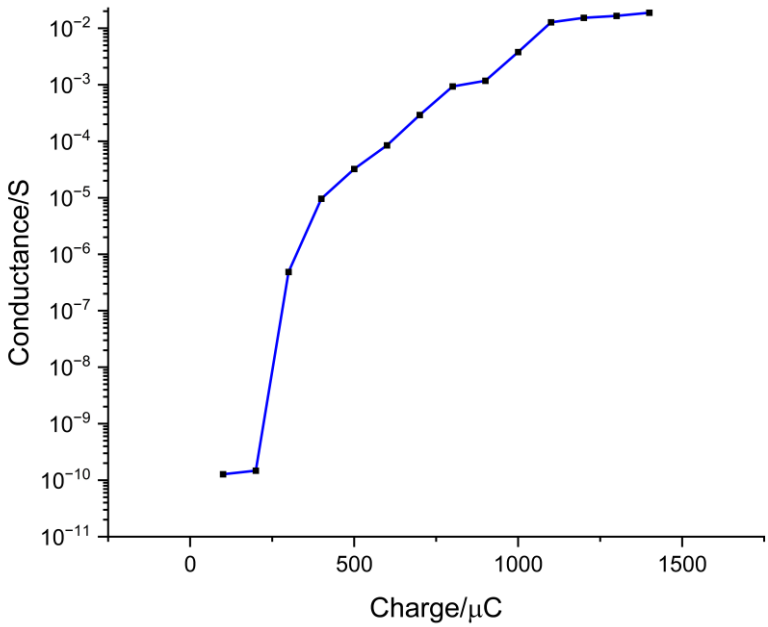

Figure 28. Explosive Percolation curve of 0.01M EDOT in BMIMPF6; RE:Ag/AgCl; WE: IDE; CE: Pt Rod, I=20uA for 5s

Performing explosive percolation method of EDOT in $BMIMFP_6$ did not yield a steep percolation region (see Figure 28). Total charge of 1000 μC was needed to attain the thin-film region which is almost double compared to acetonitrile. **Au-52** was made by delivering 400 μC of charge, which was assumed to attain percolation region.

4.8. **In-situ conductance measurement PEDOT in MeCN**

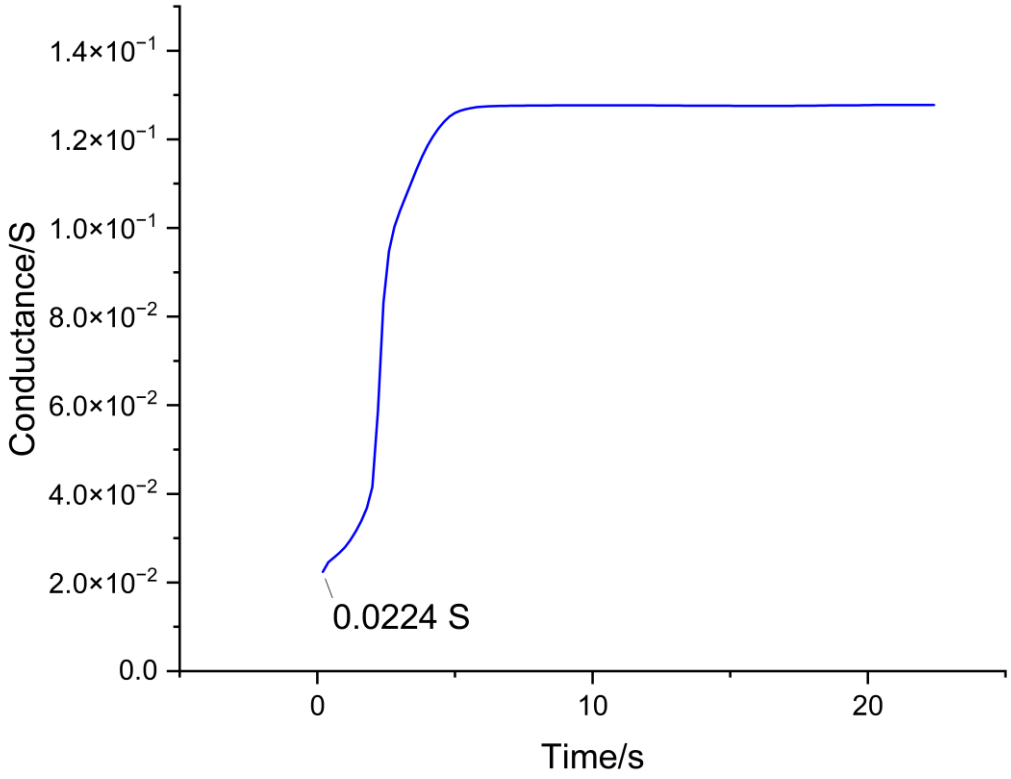

Figure 29. In-situ conductance monitoring during electropolymerization of 0.01 M EDOT in MeCN. P1: 1.0 V, P2: 0.06 V; RE: Ag/AgCl; WE: IDE; CE: Pt Rod.

A set up described in section 2.3.4 was used to perform simultaneous conductance monitoring and electropolymerization. Potentiostat P1 was used to apply potential of 1.0 V which will induce the oxidation of monomer and eventual polymer growth on IDE. Potentiostat P2 was used to apply a potential difference of 0.06 V to measure the conductance between the pads of IDE. The resulting growth curve is presented in Figure 29. Upon inspection of the growth curve, the technique is deemed not ready yet to monitor percolation curve because of its high initial conductance of 0.0224 S which, based on previous percolation curves should fall already under thin-film conductance. This conductance is combination of several resistances and capacitance present in our set up such as solution resistance, resistance of polymer between the electrodes, charge transfer resistance between the polymer and the solution, interfacial capacitance between the polymer and solution and etc. [51]. At this initial high conductance therefore, we cannot assume that components other than polymer resistance between electrodes are negligible. Kankare and Kupila circumvented this problem through

their in-house set-up and use of ac conductimetry instead of dc, this can be studied in the future [51].

PANI

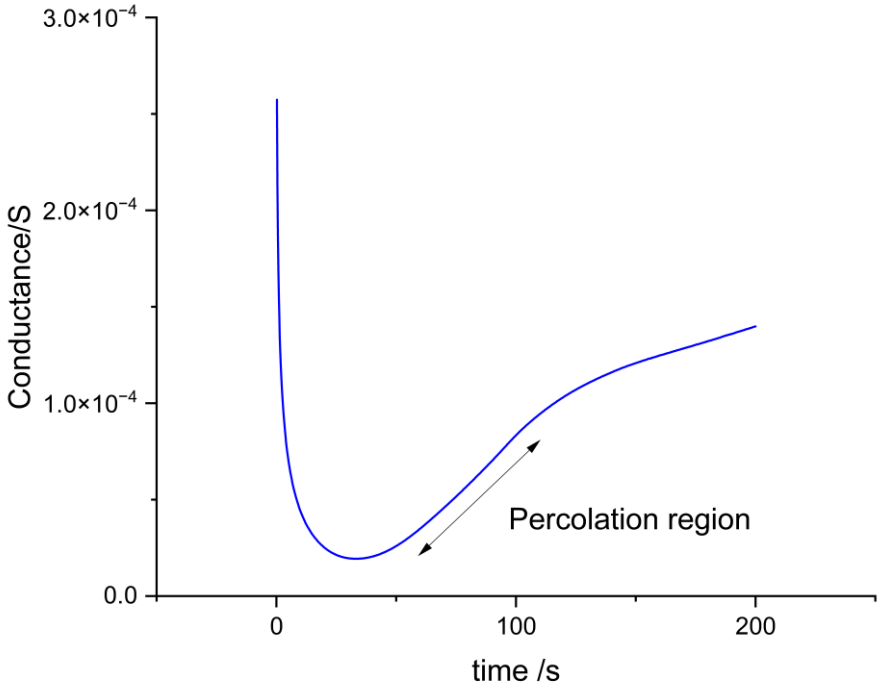

Figure 30. In-situ conductance monitoring during electropolymerization of 0.05 M Aniline in 0.5 M H_2SO_4. P1: 0.56 V, P2: 0.06 V; RE: Ag/AgCl; WE: IDE; CE: Pt Rod.

Previous potentiodynamic experiments were performed to determine the oxidation potential of aniline. It was determined to be 0.56 V and therefore the same potential was used in P1 moreover 0.06 V was applied in P2 to monitor the change in resistance between pads of IDEs in section 0. The conductance during polymer is presented in Figure 30. After 200s of polymerization the IDE was taken out of the solution and dried in the air. A 0.1 V was applied for 1 minute to IDE while in the monomer-less polymerization solution. Based on method developed by Reemts et. al [52] the resulting polymer film should be a protonated emeraldine base form. Based on Figure 30, percolation region is probably at 50-100 seconds of electropolymerization, but further experiments are needed to confirm these. The sensor produced was given an ID **Au-43.**

4.9. **Conductance in air and gas sensor response**

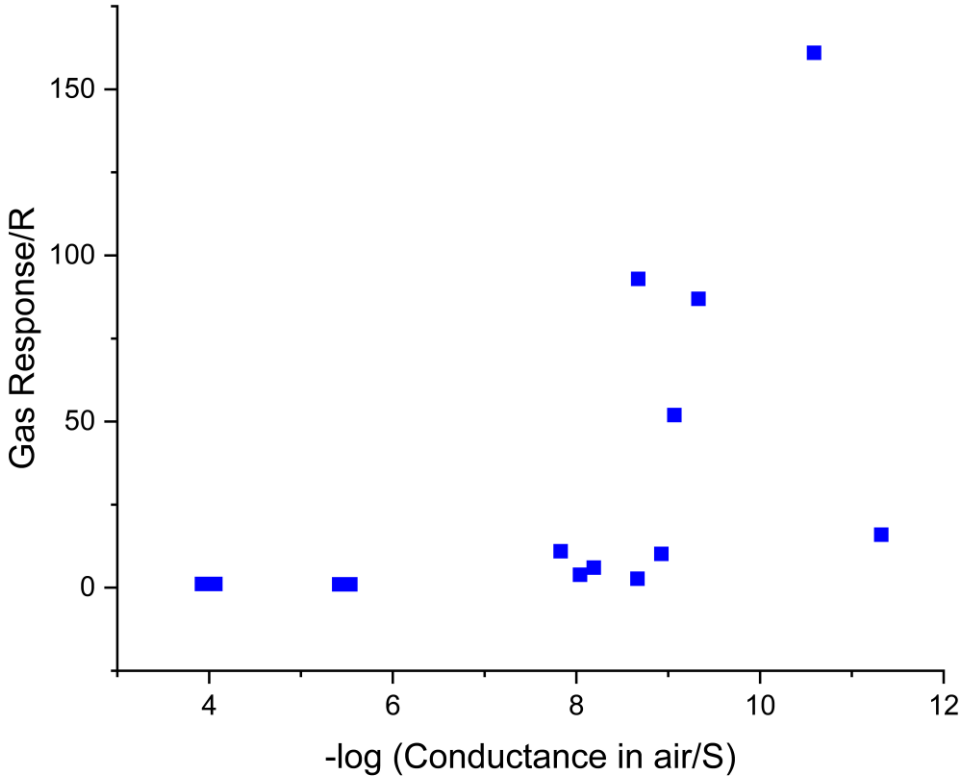

Figure 31. Relationship between gas response vs initial conductance in air. Data is from PEDOT EP sensors without p-doping.

In another effort to improve the reproducibility of the PEDOT EP sensors, several sensors were made using EP method and pulsed galvanostatic polymerization with varying amount of charge applied. The gas response to 0.005 mole fraction of ammonia in ethylene glycol were then assessed using the static odor handling set up. The concentration of ammonia used was close to the determined LOD in section 4.6. The gas response vs conductance in the air is presented in Figure 31. It was observed that the magnitude of gas response to ammonia varies inversely proportional to the initial conductance of PEDOT EP sensor, a finding which is consistent with study made by Castell et. al [16].

4.10. **Thinner PEDOT pulsed galvanostatic sensor**

Due to findings in section 4.9, much lower charge was applied while prolonging the time when the current was off to achieve lower conductance and better oxidation of the polymer [28]. Current of 20 µA for 1 s and 180 s of open cell each cycle was chosen. After 3 cycles, total charge was 60 µC. The initial conductance in the air and their gas response upon exposure to 0.005 ammonia mole fraction in ethylene glycol are presented in Table 5. Moreover, the raw signal is presented in Figure 32.

Table 5. Initial conductance and gas response to 0.005 mole fraction ammonia in ethylene glycol. Technique: Pulsed Galvanostatic polymerization; total charge 60 µC.

Sensor ID	Conductance in air, S	Gas response, R
S1	1.77E-10	304
S2	3.21E-10	83
S3	6.98E-10	47

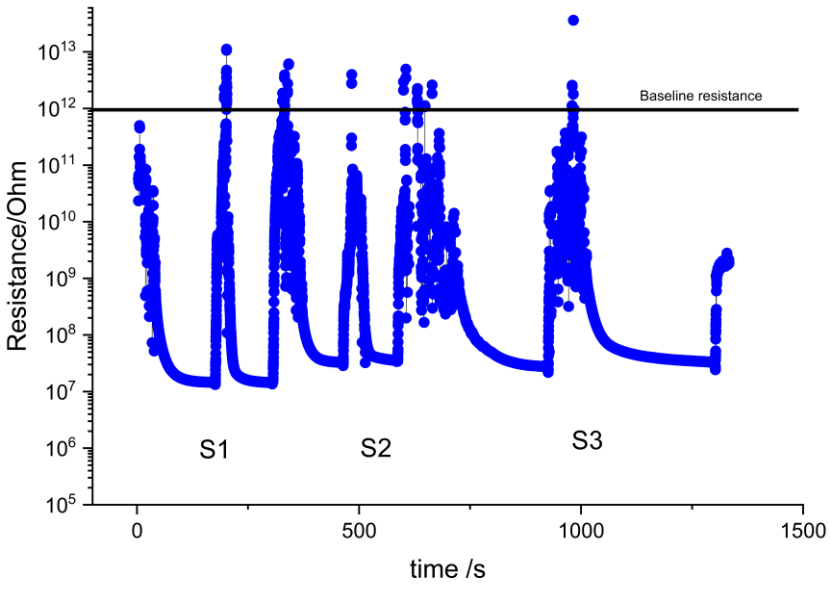

Figure 32. Raw gas sensor response of S1, S2 and S3 to 0.004 mole fraction of ammonia in ethylene glycol.

The sensors S1, S2, S3 achieved significant improvement of gas sensor response compared to the Pt-10 and Pt-14, when comparing the performance at the same concentration (0.005 NH_3

mole fraction, see Figure 23 and Figure 24). Moreover, the sensors maintained the n-type gas sensing mechanism (see Figure 32).

4.11. **Thinner PEDOT EP sensor**

To find out if the same findings can be observed in EP method of polymerization, a current of 20 µA for 1 second was passed to IDEs. The polymerization was done twice, giving the total charge of 40 µC deposited to both Pt-21 and Pt-23. Their calibration curves were presented in Figure 33 and Figure 34. The gas responses of Pt-21 and Pt-23 were much higher than Pt-10 and Pt-14 (see Figure 23 and Figure 24).

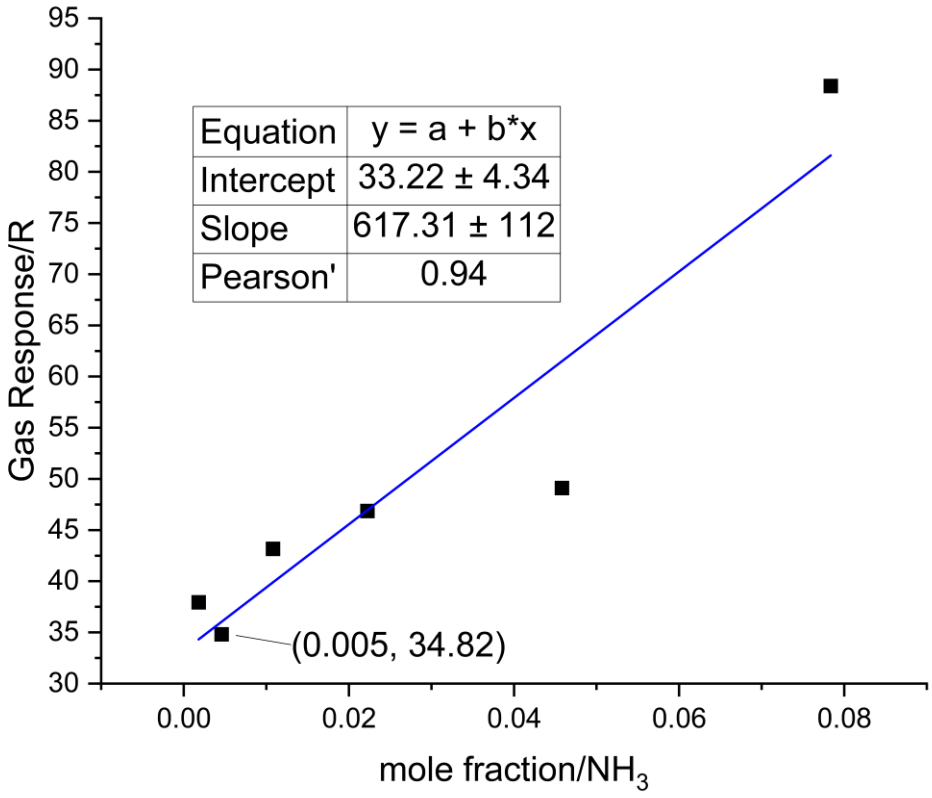

Figure 33. Pt-21 calibration curve. Highlighted point showed the gas response toward 0.005 mole fraction ammonia in ethylene glycol.

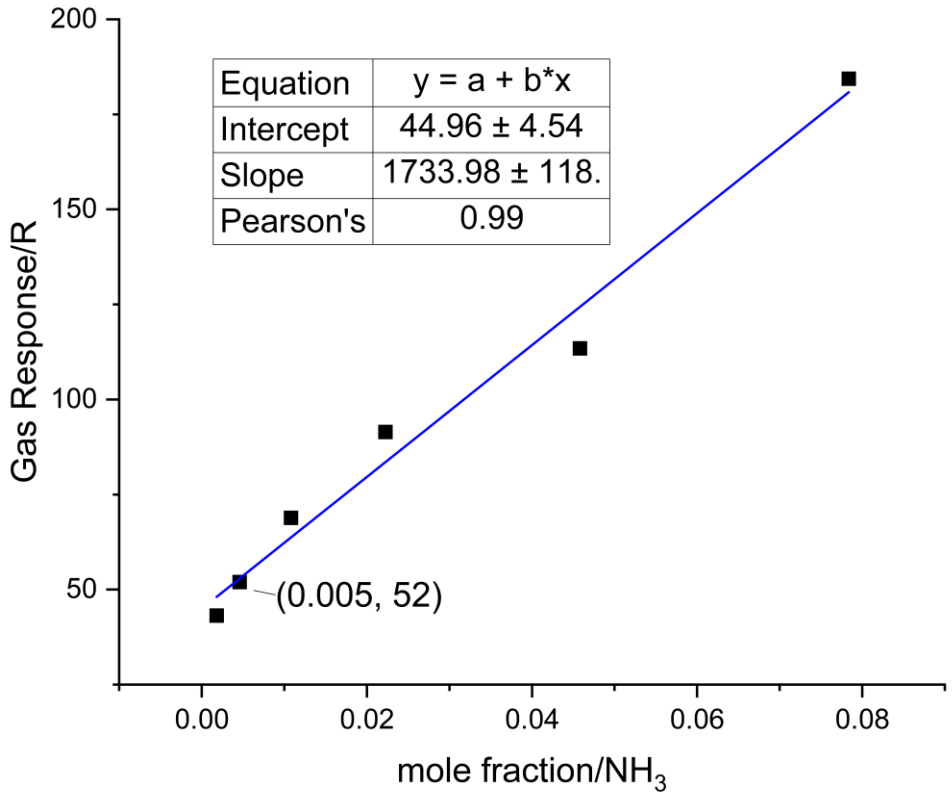

Figure 34. Pt-23 calibration curve. Highlighted point showed the gas response toward 0.005 mole fraction ammonia in ethylene glycol.

4.12. **Development of sensor array**

To create a cross-reactive sensor array one can utilize the fact that applying different electropolymerization condition such as oxidation potential, oxidant, dopant and monomer concentration can induce different morphology, conjugation length, conductivity and band gap and thus generating varying response toward number of analytes [28]. Sensors from previous experiments were used to create a sensor array and are tabulated in Table 6.

Table 6. List of sensors used to create a sensor array and its relevant information.

ID	Conducting Polymer	Electrochemical polymerization technique	Dopant	Charge or potential applied	Assumed thickness
Au-43	PANI	In-situ conductance monitoring during electro polymerization	SO_4^{2-}	Section 4.8	Thin film
S-26	PEDOT	Pulsed galvanostatic polymerization	ClO_4^-	40 µC	Percolation
S-23	PEDOT	EP method	ClO_4^-	Section 4.11	Percolation
Pt-62	PEDOT	Potentiostatic polymerization	$TFSI^-$	Section 4.7.2	Thin film
S-33	PEDOT	EP method	$TFSI^-$	40 µC	Percolation
S-8	PEDOT	EP method	ClO_4^-	60 µC	Percolation
Au-52	PEDOT	EP method	$[PF_6]^-$	Section 4.7.3	Percolation
S-10	PEDOT	Pulsed Galvanostatic polymerization	ClO_4^-	20 µC	Percolation

4.14. **Sensitivity to different VOCs**

To see if the prepared sensors respond differently to VOCs, samples were prepared by dissolving aliquot of different solvents to achieve a 0.05 mole fraction in ethylene glycol for which the total volume was 5 mL. The solution was transferred to 30-mL vial and listed sensors in Table 6 were exposed according to set-up described in section 3.4. The results are presented in Figure 35.

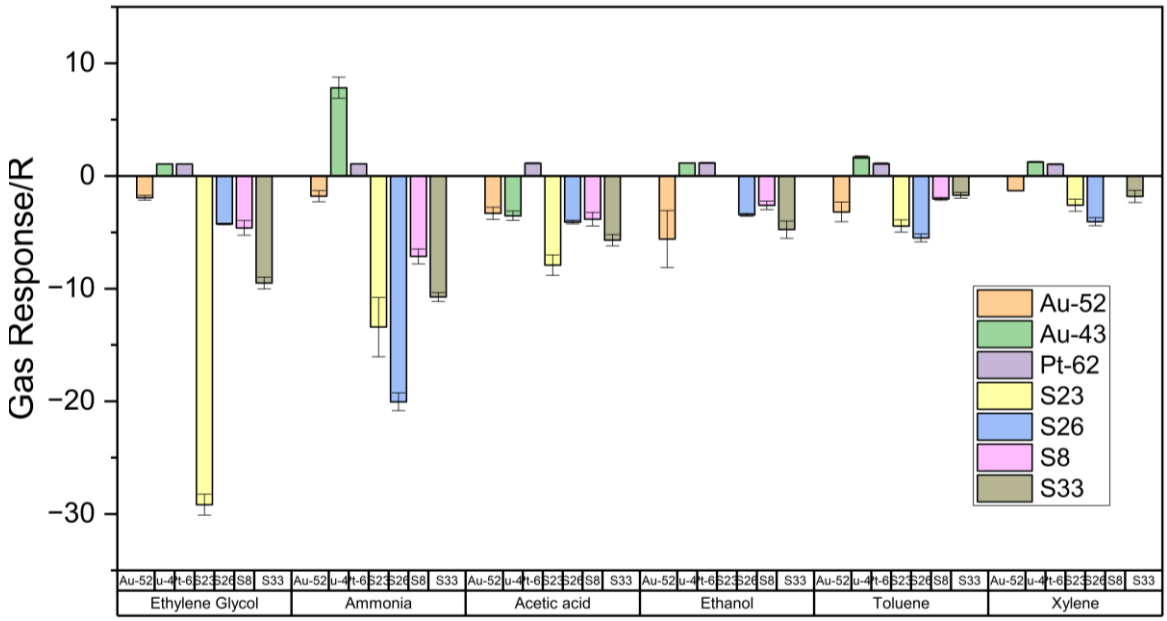

Figure 35. Gas response of sensors to ethylene glycol, ammonia, acetic acid, ethanol, toluene and xylene. Gas response of n-type sensors were multiplied by -1 to denote that the resistance decreases upon gas exposure to VOCs.

Au-43 (PANI) which is known to respond to acid-base substances showed opposite sensing behavior towards ammonia and acetic acid. Except acetic acid, it behaved as p-type material upon exposure to VOCs. Pt-62, also a thin-film sensor, also showed p-type behavior to all VOCs. Optimized sensors S8, S23, S26, and S33 from which it was made using much lower charge showed greater sensitivity (high gas response) among other sensors. Percolation sensors (Au-52, Pt-62, S23, S26, S8 and S33) outperformed thin-film sensors (Au-43 and Pt-62) in terms of intensity of gas response.

It was experimental error not to include S-10 in the measurement (see Table 6), however S-10 is most likely to exhibit same mechanism as S-26.

4.13. **Electronic nose (EN)**

Measurement order and randomization was done by assigning integer to the solvents and using the website https://www.random.org/integers/. Solvent class was assigned as *MeCN, ACE, EtOH* and *NH3* accordingly. Each vials containing the solvent was measured only once. Recorded analysis time is 240 seconds, wherein 30 seconds consists of exposing the EN system to solvent and the rest of the time is purging the system.

The dataset was partitioned into 70% training and 30% test set. Training set was then used to train the model, "mdl". An error rate of 30 % was obtained by using the trained model "mdl" in predicting the solvents in the test set. The model is the also used to predict the solvents in the whole dataset and is presented in the confusion chart (see Figure 36)

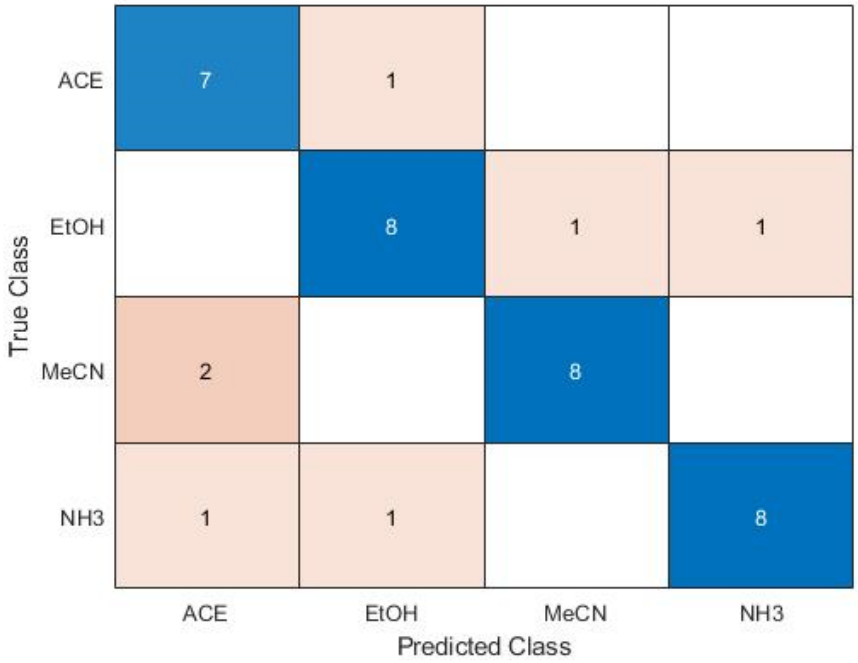

Figure 36. Confusion chart of solvent class vs the predicted solvent class by the model.

4.14. **Gas sensing mechanism of n-type PEDOT**

According to Robiños et. al, p-doping resulted in even spreading of dopant in the polymer backbone resulted in undoped PEDOT which is then become n-doped upon deprotonation of PEDOT upon exposure to ammonia. However, based on results in section 4.5, 4.10 and 4.11 we've seen that the sensors maintained the n-type mechanism even without p-doping. Moreover, there's no ionizable proton in PEDOT backbone (see Figure 4) to be protonated.

Therefore, a new mechanism is proposed which is based on the formation of an overoxidized PEDOT.

According to Castell et. Al, when PEDOT is exposed to strong oxidizing agent like NO_2, the film undergoes next stage overoxidation, causing increase in resistance upon exposure to NO_2 a characteristic of a n-type material [53]. Exposure to electron donating substance like ammonia will therefore result in decrease in resistance. This proposed mechanism is supported by the fact that overoxidation increases the Fermi level in PEDOT: PSS and at working on potential 1.1-1.5 V promotes simultaneously polymer growth and overoxidation. During initial stages of pulsed galvanostatic polymerization (see Figure 20) the ratio of overoxidized to pristine PEDOT is high therefore the n-type mechanism (S8, S23, S26, and S33) prevails but as the polymerization continue the potential needed to sustain polymer growth decreases so as the prevalence of overoxidation therefore the p-type mechanism prevails (Pt-62, Figure 35). This however needs to confirm from infrared spectroscopy experiments.

5. Conclusion

In this master's thesis, a potentiostatic and galvanostatic polymerization using EP method revealed the underlying repeatability issue of working in the percolation regime. A pulsed galvanostatic polymerization was employed in order to address the problem. This method also rendered non-repeatable results however, Pt-10 and Pt-14 sensors that were made using this method showed n-type gas sensing mechanism without employing p-doping. Moreover, these sensors showed high linearity range, high sensitivity, and low detection limits.

In search for a wider application of EP method, electropolymerization of PEDOT was investigated in ionic liquids. A percolation growth curve was successfully achieved in ionic liquids; however, mass transfer limiting polymerization was observed due to IL high viscosity.

High initial conductance was realized during in-situ conductance monitoring during electropolymerization which makes it difficult to study the percolation region in both acetonitrile and ionic liquids. Nevertheless, it is successful in producing a thin-film PANI.

Inverse correlation of initial conductance to the magnitude of gas response was observed which led to producing thinner percolation network sensors. These sensors achieved a higher gas response compared to Pt-10 and Pt-14, while maintaining the n-type gas sensing mechanism.

Exposure to VOCs confirmed the acid-base gas sensing mechanism of PANI, n-type mechanism of EP method and pulsed galvanostatic method sensors while p-type mechanism for thin-film sensor.

A new gas sensing mechanism was proposed for the n-type PEDOT sensor which is based on a ratio of overoxidized PEDOT to pristine PEDOT.

Several sensors which have varying dopant, solvent, thickness, and mostly likely morphology due to varying electrochemical techniques employed were produced throughout the study. These sensors were used to create an electronic nose system which gave a 70% accuracy rate in predicting solvent class of acetonitrile, ethanol, methanol and ammonia.

6. References

[1] J. Green, A. Doble, J. Bartl, How a kingfisher helped reshape Japan's bullet train, BBC News. (2019). https://www.bbc.com/news/av/science-environment-47673287.

[2] C. Hurot, N. Scaramozzino, A. Buhot, Y. Hou, Bio-inspired strategies for improving the selectivity and sensitivity of artificial noses: A review, Sens. Switz. 20 (2020) 1–28. https://doi.org/10.3390/s20061803.

[3] S.S. Schiffman, T.C. Pearce, Introduction to Olfaction: Perception, Anatomy, Physiology, and Molecular Biology, in: Handb. Mach. Olfaction, 2002: pp. 1–31. https://doi.org/10.1002/3527601597.ch1.

[4] S.Y. Park, Y. Kim, T. Kim, T.H. Eom, S.Y. Kim, H.W. Jang, Chemoresistive materials for electronic nose: Progress, perspectives, and challenges, InfoMat. 1 (2019) 289–316. https://doi.org/10.1002/inf2.12029.

[5] M.A. Ryan, H. Zhou, Automotive and Aerospace Applications, in: Handb. Mach. Olfaction, 2002: pp. 525–546. https://doi.org/10.1002/3527601597.ch22.

[6] C. Di Natale, R. Paolesse, A. D'Amico, Food and Beverage Quality Assurance, in: Handb. Mach. Olfaction, 2002: pp. 505–524. https://doi.org/10.1002/3527601597.ch21.

[7] T. Bachinger, J.-E. Haugen, Process Monitoring, in: Handb. Mach. Olfaction, 2002: pp. 481–503. https://doi.org/10.1002/3527601597.ch20.

[8] H.T. Nagle, R. Gutierrez-Osuna, B.G. Kermani, S.S. Schiffman, Environmental Monitoring, in: Handb. Mach. Olfaction, 2002: pp. 419–444. https://doi.org/10.1002/3527601597.ch17.

[9] P.A. Rodriguez, T.T. Tan, H. Gygax, Cosmetics and Fragrances, in: Handb. Mach. Olfaction, 2002: pp. 561–577. https://doi.org/10.1002/3527601597.ch24.

[10] O. Deffenderfer, S. Feast, F.-X. Garneau, Recognition of Natural Products, in: Handb. Mach. Olfaction, 2002: pp. 461–480. https://doi.org/10.1002/3527601597.ch19.

[11] V.K. Pamula, Detection of Explosives, in: Handb. Mach. Olfaction, 2002: pp. 547–560. https://doi.org/10.1002/3527601597.ch23.

[12] K.C. Persaud, A.M. Pisanelli, P. Evans, Medical Diagnostics and Health Monitoring, in: Handb. Mach. Olfaction, 2002: pp. 445–460. https://doi.org/10.1002/3527601597.ch18.

[13] A. Sierra-Padilla, J.J. García-Guzmán, D. López-Iglesias, J.M. Palacios-Santander, L. Cubillana-Aguilera, E-Tongues/Noses Based on Conducting Polymers and Composite Materials: Expanding the Possibilities in Complex Analytical Sensing, Sensors. 21 (2021) 4976. https://doi.org/10.3390/s21154976.

[14] Y.C. Wong, B.C. Ang, A.S.M.A. Haseeb, A.A. Baharuddin, Y.H. Wong, Review—Conducting Polymers as Chemiresistive Gas Sensing Materials: A Review, J. Electrochem. Soc. 167 (2020) 037503. https://doi.org/10.1149/2.0032003jes.

[15] K. Murugappan, M.R. Castell, Bridging electrode gaps with conducting polymers around the electrical percolation threshold, Electrochem. Commun. 87 (2018) 40–43. https://doi.org/10.1016/j.elecom.2017.12.019.

[16] B. Armitage, K. Murugappan, M. Lefferts, A. Cowsik, M. Castell, Conducting polymer percolation gas sensor on a flexible substrate, J. Mater. Chem. C. 8 (2020) 12669–12676. https://doi.org/10.1039/d0tc02856h.

[17] Å.A. University, A. Robiños, CONDUCTING POLYMER NETWORKS AT EXPLOSIVE PERCOLATION REGION: ULTRA-FAST RESPONSE AND RECOVERY GAS SENSORS AT ROOM TEMPERATURE, 2022.

[18] W.S. Li, M.J. Lefferts, B. Armitage, K. Murugappan, M.R. Castell, Polypyrrole Percolation Network Gas Sensors: Improved Reproducibility through Conductance Monitoring during Polymer Growth, ACS Appl. Polym. Mater. 4 (2022) 2536–2543. https://doi.org/10.1021/acsapm.1c01819.

[19] J. Janata, Principles of Chemical Sensors, (2009). https://doi.org/10.1007/b136378.
[20] H. Bai, G. Shi, Gas Sensors Based on Conducting Polymers, (2007) 41.
[21] P. Chandrasekhar, Conducting Polymers, Fundamentals and Applications, Springer International Publishing, 2018. https://doi.org/10.1007/978-3-319-69378-1.
[22] M.O. Farea, H.A. Alhadlaq, Z.M. Alaizeri, A.A.A. Ahmed, M.O. Sallam, M. Ahamed, High Performance of Carbon Monoxide Gas Sensor Based on a Novel PEDOT:PSS/PPA Nanocomposite, ACS Omega. 7 (2022) 22492–22499. https://doi.org/10.1021/acsomega.2c01664.
[23] S. Nie, Z. Li, Y. Yao, Y. Jin, Progress in Synthesis of Conductive Polymer Poly(3,4-Ethylenedioxythiophene), Front. Chem. 9 (2021) 803509. https://doi.org/10.3389/fchem.2021.803509.
[24] M. Ren, H. Zhou, H.-J. Zhai, Obvious enhancement in electrochemical capacitive properties for poly(3,4-ethylenedioxythiophene) electrodes prepared under optimized conditions, J. Mater. Sci. Mater. Electron. 32 (2021) 10078–10088. https://doi.org/10.1007/s10854-021-05666-3.
[25] Zh.A. Boeva, V.G. Sergeyev, Polyaniline: Synthesis, properties, and application, Polym. Sci. Ser. C. 56 (2014) 144–153. https://doi.org/10.1134/S1811238214010032.
[26] A.H. Majeed, L.A. Mohammed, O.G. Hammoodi, S. Sehgal, M.A. Alheety, K.K. Saxena, S.A. Dadoosh, I.K. Mohammed, M.M. Jasim, N.U. Salmaan, A Review on Polyaniline: Synthesis, Properties, Nanocomposites, and Electrochemical Applications, Int. J. Polym. Sci. 2022 (2022) 1–19. https://doi.org/10.1155/2022/9047554.
[27] I. Fratoddi, I. Venditti, C. Cametti, M.V. Russo, Chemiresistive polyaniline-based gas sensors: A mini review, Sens. Actuators B Chem. 220 (2015) 534–548. https://doi.org/10.1016/j.snb.2015.05.107.
[28] S. Cosnier, A. Karyakin, eds., Electropolymerization: Concepts, Materials and Applications, Wiley-VCH Verlag GmbH & Co. KGaA, Weinheim, Germany, 2010. https://doi.org/10.1002/9783527630592.
[29] T.F. Fuller, J.N. Harb, Electrochemical engineering, First edition, Wiley, Hoboken, NJ, USA, 2018.
[30] G. Inzelt, Conducting polymers: a new era in electrochemistry, Springer, Berlin, 2008.
[31] J. Unsworth, B.A. Lunn, P.C. Innis, Z. Jin, A. Kaynak, N.G. Booth, Technical Review : Conducting Polymer Electronics, J. Intell. Mater. Syst. Struct. 3 (1992) 380–395. https://doi.org/10.1177/1045389X9200300301.
[32] G.P. Pandey, A.C. Rastogi, Synthesis and characterization of pulsed polymerized poly(3,4-ethylenedioxythiophene) electrodes for high-performance electrochemical capacitors, Electrochimica Acta. 87 (2013) 158–168. https://doi.org/10.1016/j.electacta.2012.08.125.
[33] G. Salinas, B.A. Frontana-Uribe, Analysis of Conjugated Polymers Conductivity by in situ Electrochemical-Conductance Method, ChemElectroChem. 6 (2019) 4105–4117. https://doi.org/10.1002/celc.201801488.
[34] B. Eggins, Chemical Sensors and Biosensors, 2007. https://doi.org/10.1002/9780470511305.
[35] G. Korotcenkov, Metal oxides for solid-state gas sensors: What determines our choice?, Mater. Sci. Eng. B Solid-State Mater. Adv. Technol. 139 (2007) 1–23. https://doi.org/10.1016/j.mseb.2007.01.044.
[36] M. Tonezzer, L. Van Duy, Gas Sensors, in: Encycl. Sens. Biosens., Elsevier, 2023: pp. 185–208. https://doi.org/10.1016/B978-0-12-822548-6.00113-8.
[37] P. Kubisa, Ionic liquids in the synthesis and modification of polymers, J. Polym. Sci. Part Polym. Chem. 43 (2005) 4675–4683. https://doi.org/10.1002/pola.20971.

[38] J.M. Pringle, J. Efthimiadis, P.C. Howlett, J. Efthimiadis, D.R. MacFarlane, A.B. Chaplin, S.B. Hall, D.L. Officer, G.G. Wallace, M. Forsyth, Electrochemical synthesis of polypyrrole in ionic liquids, Polymer. 45 (2004) 1447–1453. https://doi.org/10.1016/j.polymer.2004.01.006.
[39] T. Sauerwald, S. Russ, Percolation Effects in Metal Oxide Gas Sensors and Related Systems, in: C.-D. Kohl, T. Wagner (Eds.), Gas Sens. Fundam., Springer Berlin Heidelberg, Berlin, Heidelberg, 2013: pp. 247–278. https://doi.org/10.1007/5346_2013_53.
[40] D. Stauffer, A. Aharony, Introduction to Percolation Theory, 0 ed., Taylor & Francis, 2018. https://doi.org/10.1201/9781315274386.
[41] Christensen, Kim, Percolation Theory, (2002). https://web.mit.edu/ceder/publications/Percolation.pdf (accessed June 22, 2023).
[42] N. Bastas, P. Giazitzidis, M. Maragakis, K. Kosmidis, Explosive percolation: Unusual transitions of a simple model, Phys. Stat. Mech. Its Appl. 407 (2014) 54–65. https://doi.org/10.1016/j.physa.2014.03.085.
[43] T.C. Pearce, S.S. Schiffman, H.T. Nagle, J.W. Gardner, eds., Handbook of Machine Olfaction: Electronic Nose Technology, 1st ed., Wiley, 2002. https://doi.org/10.1002/3527601597.
[44] Y.Y. Broza, H. Haick, Nanomaterial-based sensors for detection of disease by volatile organic compounds, Nanomed. 8 (2013) 785–806. https://doi.org/10.2217/nnm.13.64.
[45] J. Yan, X. Guo, S. Duan, P. Jia, L. Wang, C. Peng, S. Zhang, Electronic Nose Feature Extraction Methods: A Review, Sensors. 15 (2015) 27804–27831. https://doi.org/10.3390/s151127804.
[46] S.M. Scott, D. James, Z. Ali, Data analysis for electronic nose systems, Microchim. Acta. 156 (2006) 183–207. https://doi.org/10.1007/s00604-006-0623-9.
[47] MX-ED-IDE3-Pt, n.d. https://www.basinc.com/products/MX-ED-IDE3-Pt.
[48] Micrux Technologies, Thin-film InterDigitated Electrodes - Micrux Fluidic - PDF Catalogs | Technical Documentation | Brochure, (n.d.). https://pdf.directindustry.com/pdf/micrux-fluidic/thin-film-interdigitated-electrodes/240350-975916.html.
[49] A.I. Melato, M.H. Mendonça, L.M. Abrantes, Effect of the electropolymerisation conditions on the electrochemical, morphological and structural properties of PEDOTh films, J. Solid State Electrochem. 13 (2009) 417–426. https://doi.org/10.1007/s10008-008-0522-6.
[50] A. Ejigu, K.R.J. Lovelock, P. Licence, D.A. Walsh, Iodide/triiodide electrochemistry in ionic liquids: Effect of viscosity on mass transport, voltammetry and scanning electrochemical microscopy, Electrochimica Acta. 56 (2011) 10313–10320. https://doi.org/10.1016/j.electacta.2011.03.108.
[51] J. Kankare, E.-L. Kupila, In-situ conductance measurement during electropolymerization, J. Electroanal. Chem. 322 (1992) 167–181. https://doi.org/10.1016/0022-0728(92)80074-E.
[52] J. Reemts, J. Parisi, D. Schlettwein, Electrochemical growth of gas-sensitive polyaniline thin films across an insulating gap, Thin Solid Films. 466 (2004) 320–325. https://doi.org/10.1016/j.tsf.2004.03.010.
[53] M.J. Lefferts, B. Armitage, K. Murugappan, M.R. Castell, PEDOT percolation networks for reversible chemiresistive sensing of NO2, RSC Adv. 11 (2021) 22789–22797. https://doi.org/10.1039/d1ra03648c.

7. Appendix

The following code were used to classify solvent:

```
SolventData.Class = categorical(SolventData.Class);

pt = cvpartition(SolventData.Class,"HoldOut",0.3);

SolventTrain = SolventData(training(pt),:);

SolventTest = SolventData(test(pt),:)

mdl = fitcdiscr(SolventTrain,"Class");

errRate = loss(mdl,SolventTest);

predLabel = predict(mdl,SolventData);

confusionchart(SolventData.Class,predLabel)
```